MSR in Diamond

SH Connell, K Bharuth-Ram, S Cox

University of Johannesburg, Univ. of KwaZulu-Natal, Rutherford Appleton Lab

1. Natural diamond
2. Synthetic Diamond
3. Synchrotron characterisation
4. Muon Spin Rotation studies
5. Coherence

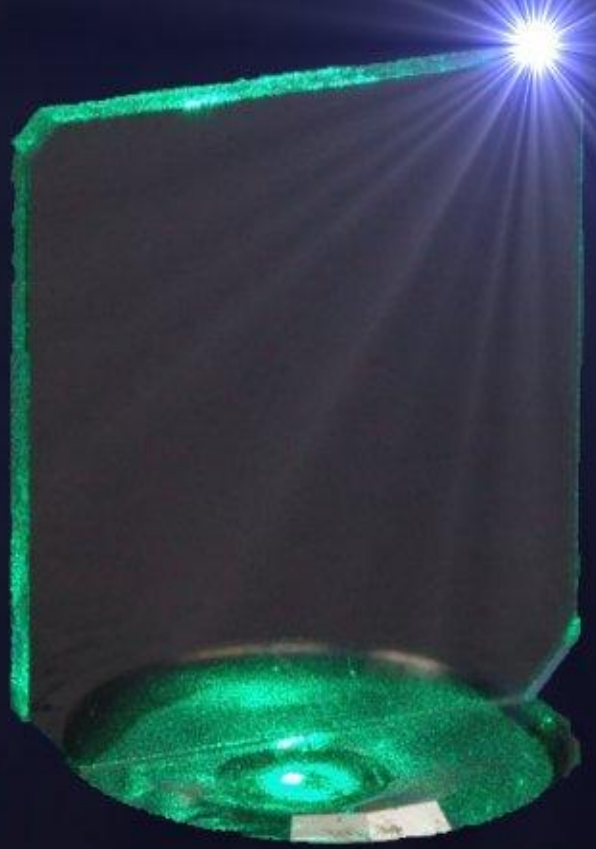

Photograph by James Nachtwey

SOUTH AFRICA. JUNE 2010

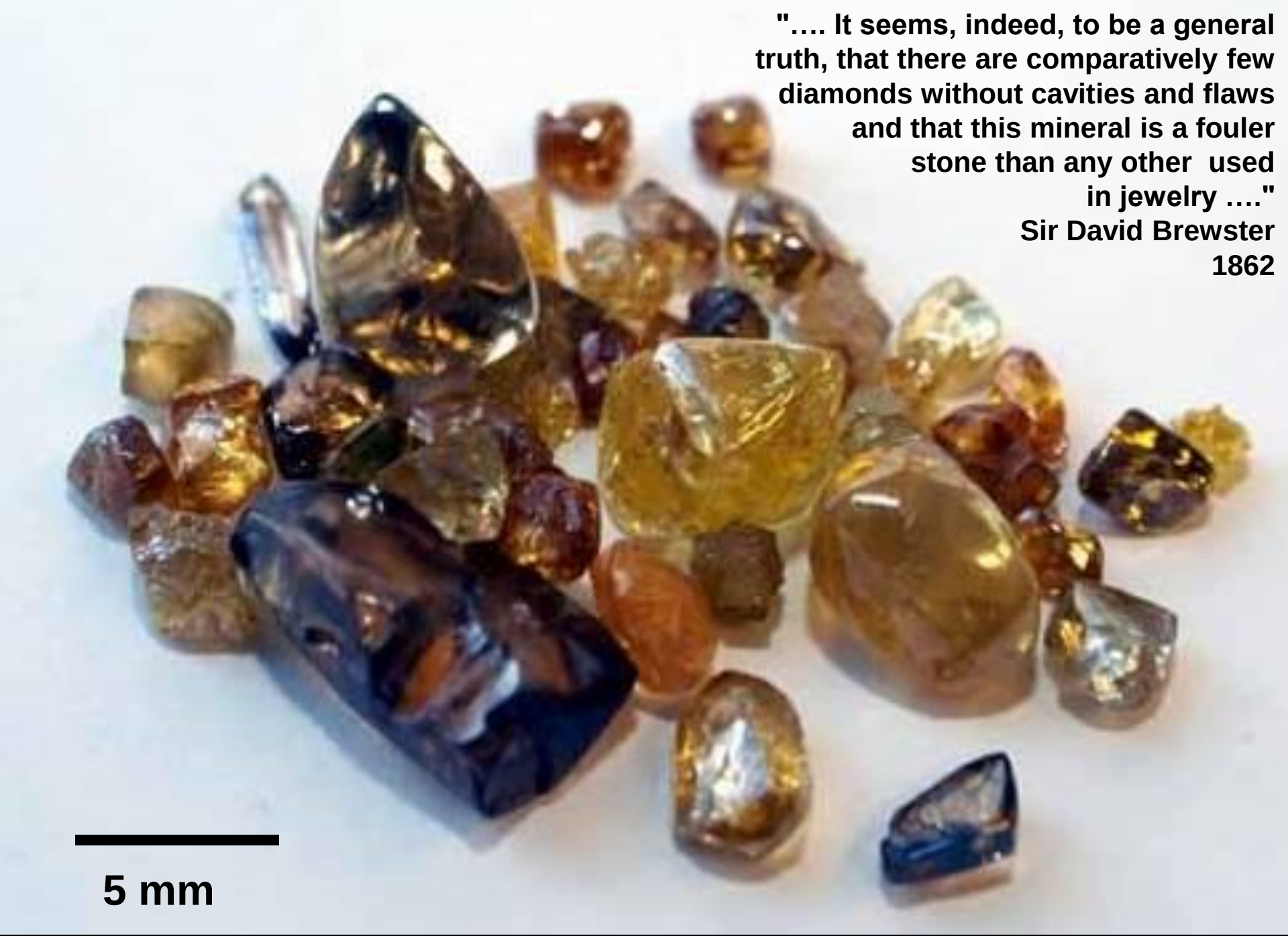

Courtesy J Hansen - Hansen Future Materials

This is all changing …….

… diamond for high tech applications

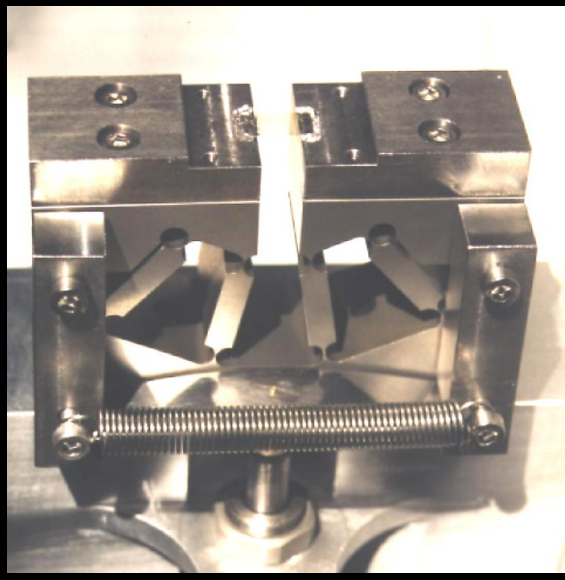

“ … the dawn of diamond electronics has arrived …"
Element Six MD, Christian Hultner 24-02-2005

“… a crucial new role for diamond in an ultra-high technology area is emerging …”
SYNCHROTRON RADIATION NEWS, Vol. 18, No. 1, 2005

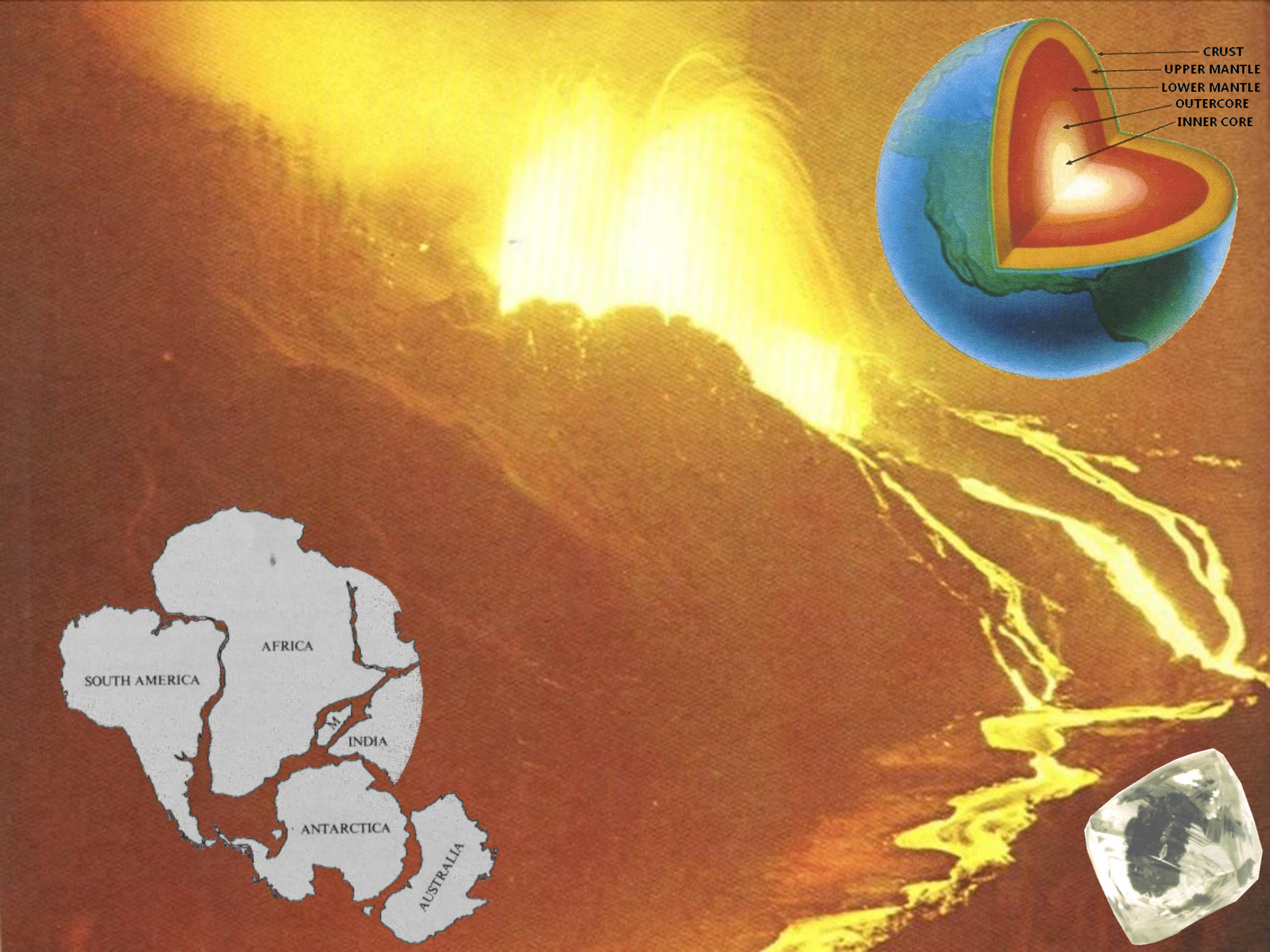
CRUST
UPPER MANTLE
LOWER MANTLE
OUTERCORE
INNER CORE
AFRICA
SOUTH AMERICA
INDIA
ANTARCTICA
AUSTRALIA

Diamond

IR Spectra

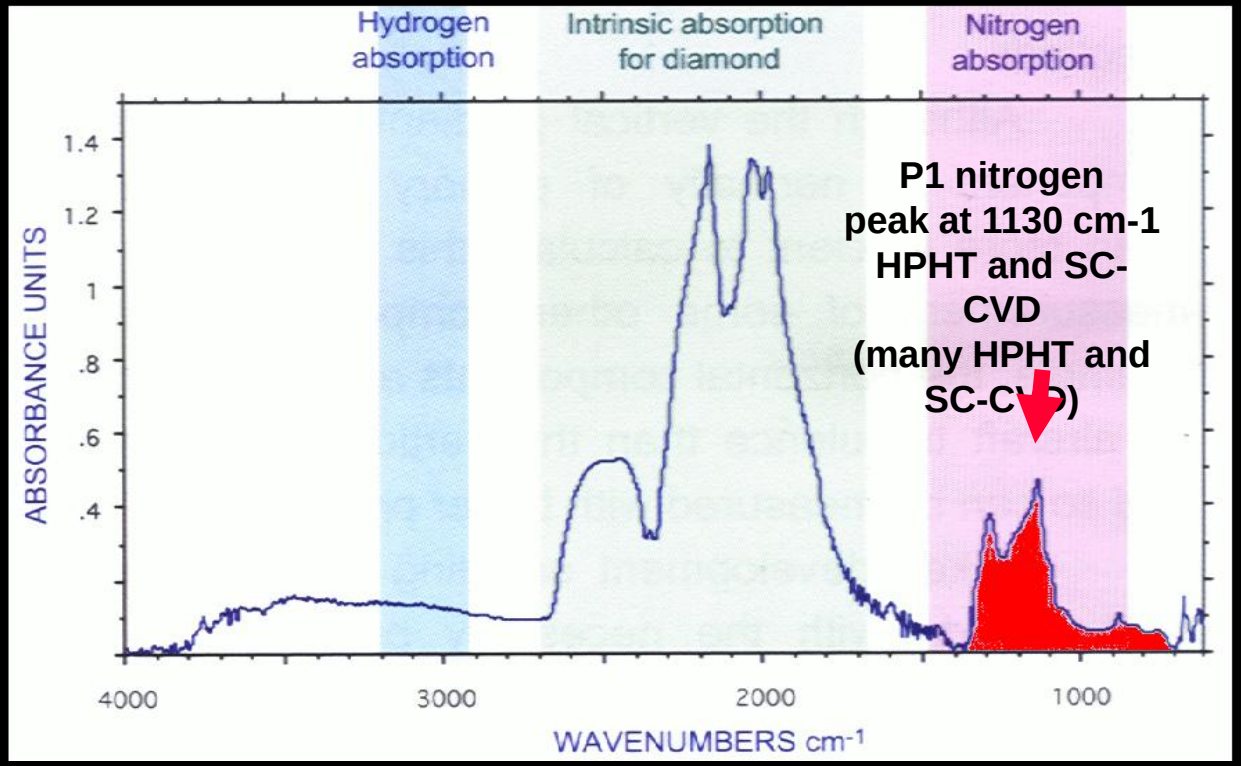

Consider absorption, luminescence and EPR centres
Very complex …..

Number	Year	Reference
123	1990	F Bridges et al in J. Phys Cond. Mat.,2 (1990) 2875-2928
300+	1998	AM Zaitsev et al in Handbook of Industrial Diamond and Diamond Films, Dekker, New York, (1998)

CVD diamond

Properties (at best)

1. Substitutional N, B < few ppb
2. CCD ~ 1mm
3. Combined mobility ~ theoretical
4. Best case : Residual strain ~ 10^{-6}
5. Plates 5 – 10 mm sides

Electronic grade SC-CVD
(~100 GBP /mm³)

Optical grade PC-CVD
(~25 GBP /mm³)

Nano diamond
(~1 $ /cm³)

HPHT diamond

Properties (at best)

1. Substitutional N, B ~ few ppb
2. Best case : Residual strain ~ 10^{-8}
3. Plates 5 – 10 mm sides

Low Strain IIa HPHT

(~1000 €/mm³)

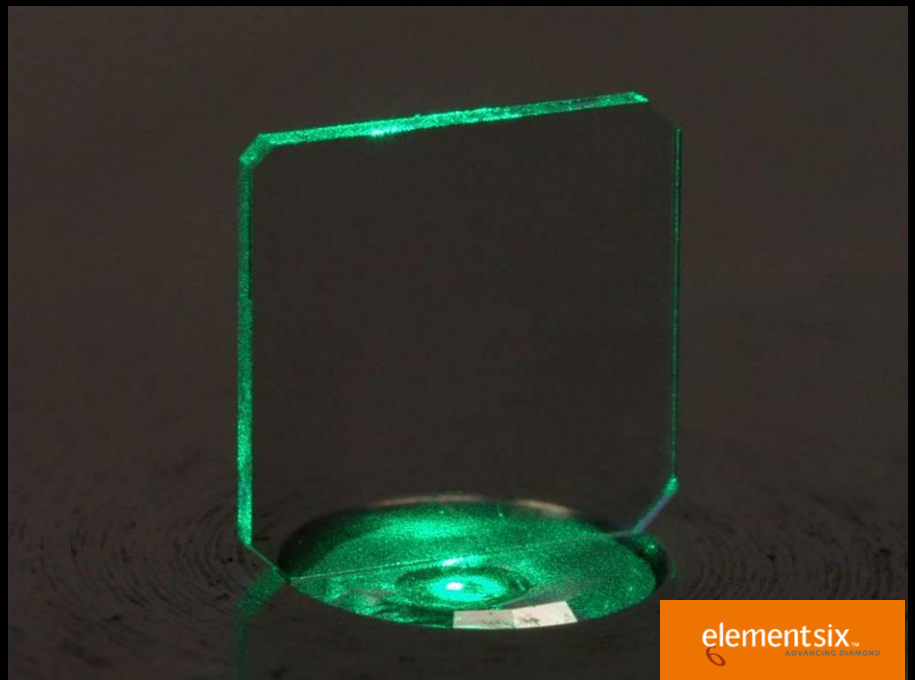

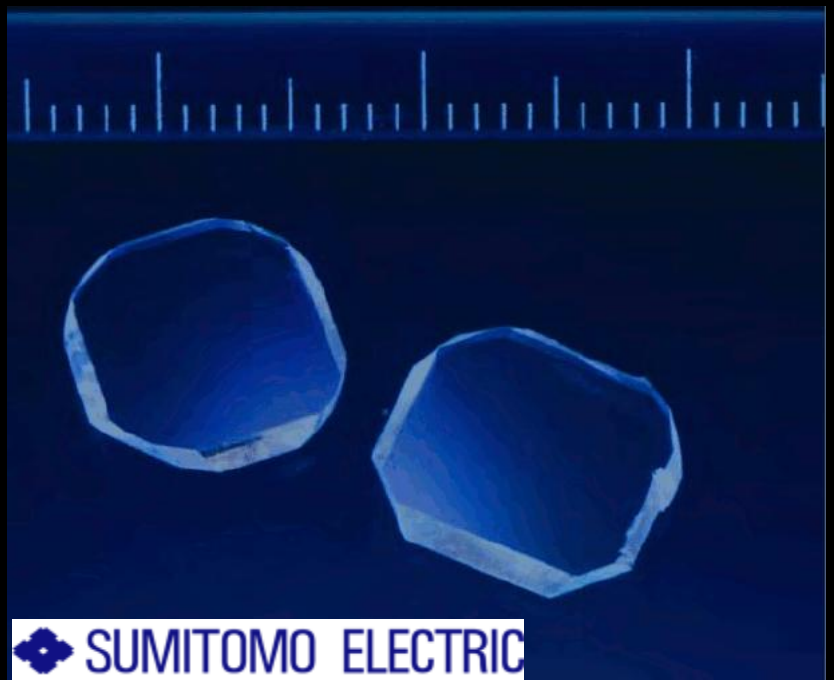

“Electronic" diamond

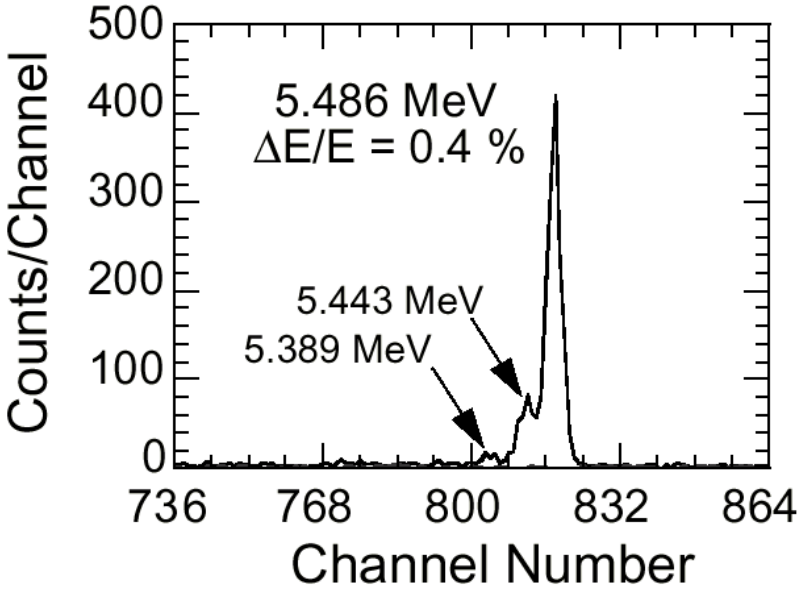

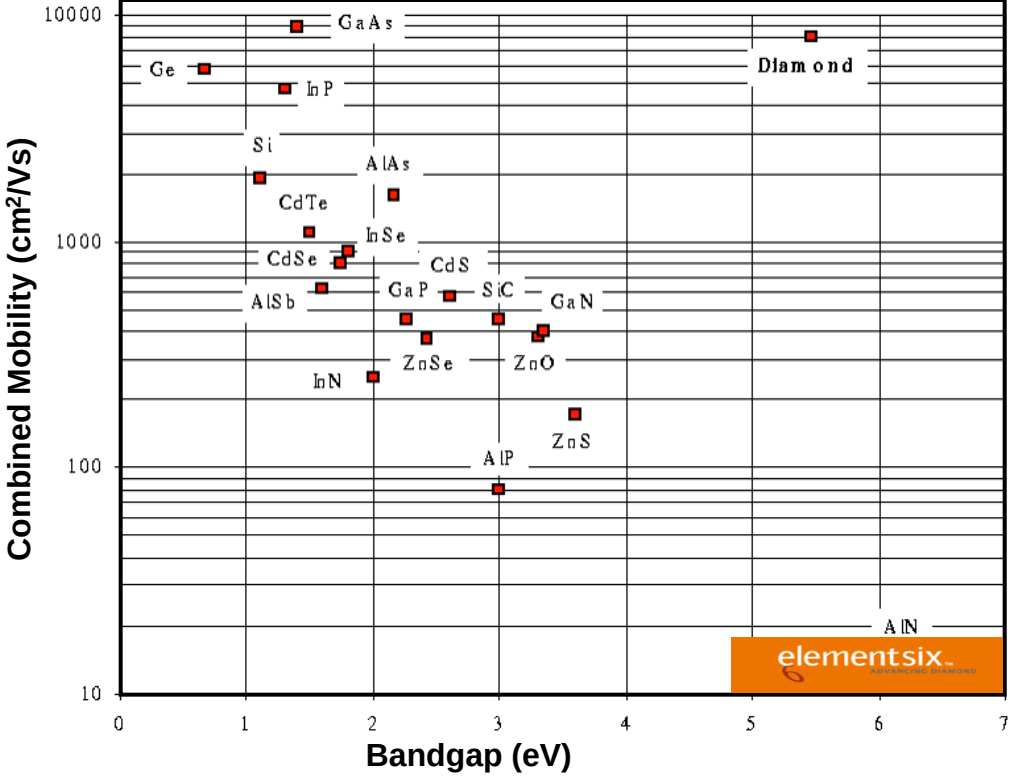

τ > 2 µs, CCD > $\Delta x_{material}$

μ_c high combined mobility,
ε_g wide band gap,
E_b high breakdown field,
Ω high resistivity
σ high thermal conductivity,
$\Delta\lambda$ broad spectral band,
ε_r low relative permeability
n_v very radiation hard

FoM
(various)

Diamond >> Si
8000 x

✓ **Intrinsic**
✓ **p-type**
? … **n-type**

Study

- **Charge carrier dynamics**
- **Near surface defects**
- **Contacts**
- **Electrically active defects**

“Optical” Diamond

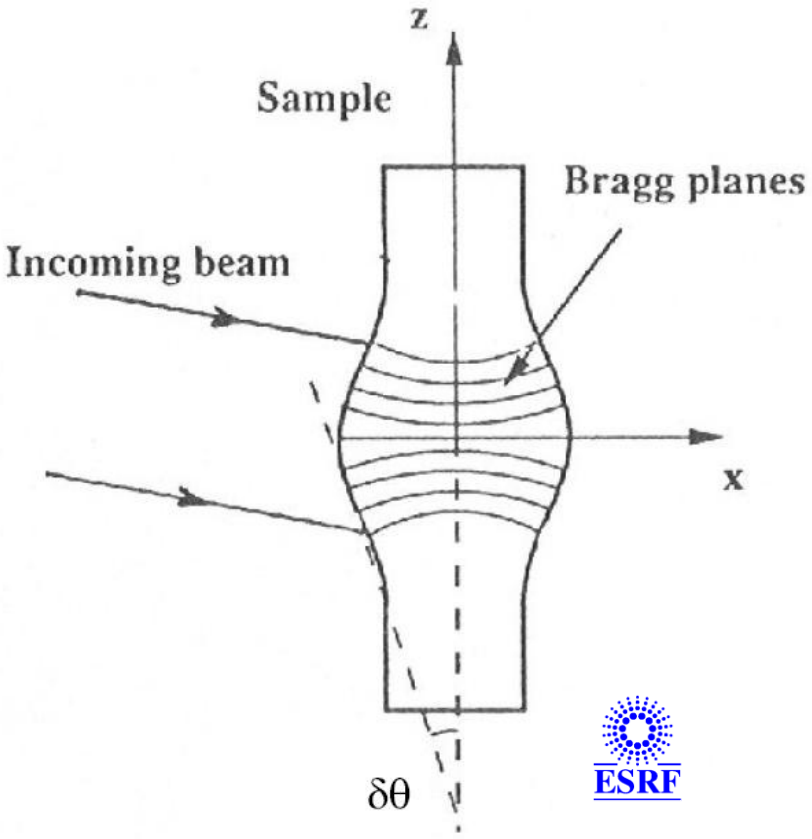

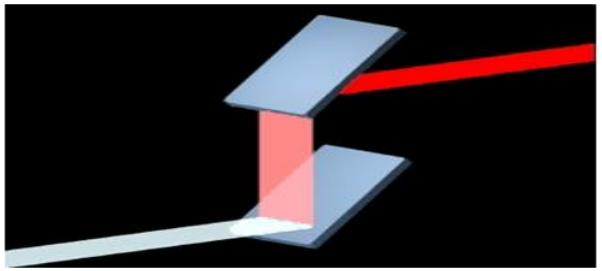

Eg. Monochromator for Synchrotron X-rays

- σ **high thermal conductivity,**
- μ **low linear X-ray absorption,**
- α **low thermal expansion**

$$\delta\theta \propto \left(\frac{\sigma}{\mu\alpha}\right)^{-1}$$

Diamond >> Silicon

500 x

For Silicon :
liquid N_2 cooling works up to 400 W/mm^2

For FEL’s: 10-100 GW/pulse (t_{pulse} = 100fs)
Response to transients important

Thermal	Diamond (0.07% ^{13}C)	Silicon	Copper
Diffusivity (cm^2/s)	18.5	0.86	1.25

Improvements in Diamond Synthesis

Increasing quality

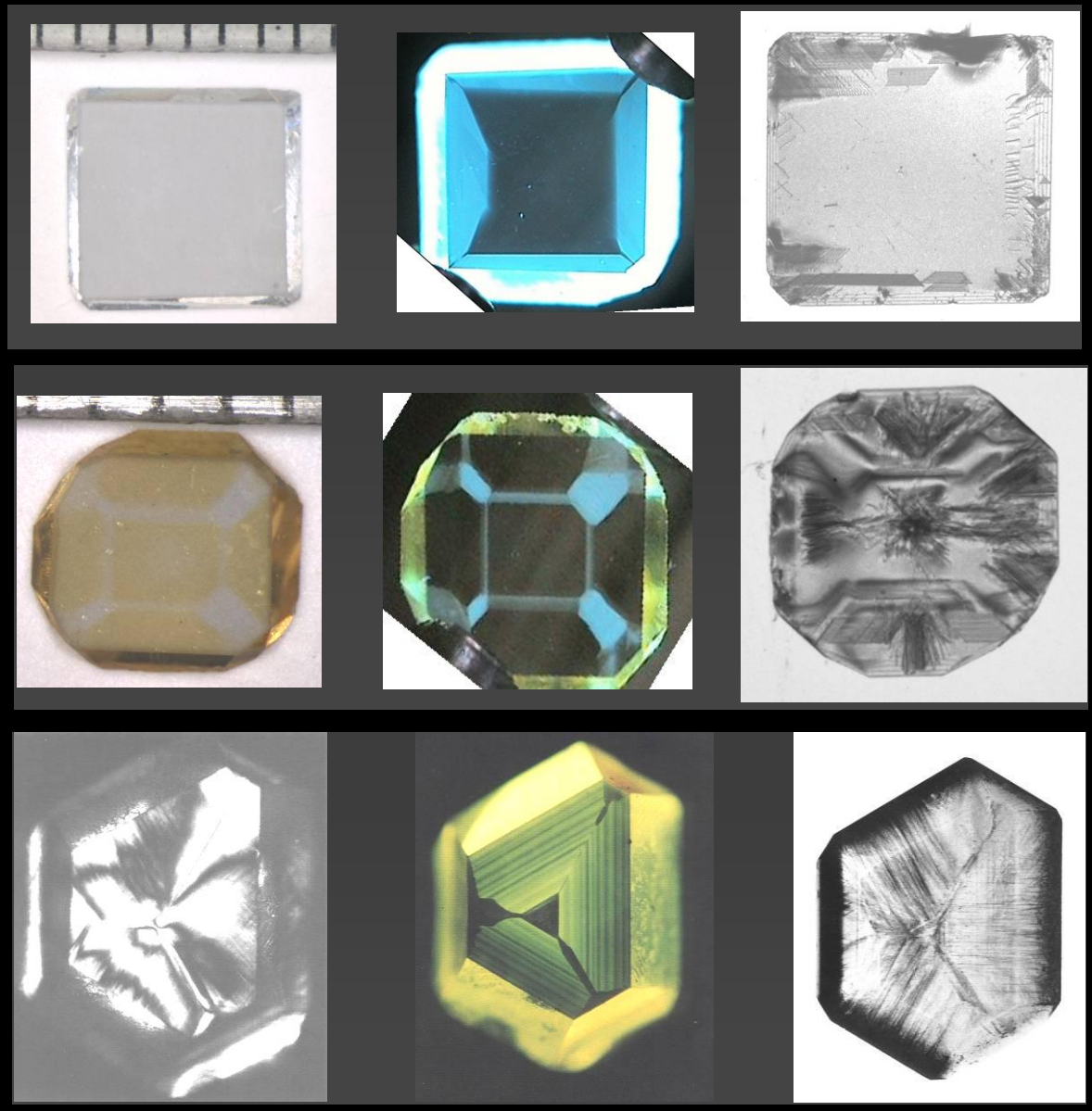

Optical microscope

UV luminescence

White beam topograph


30/11/05
20
21
22
23
24
25
26
Courtesy J Hansen -
Hansen Future Materials

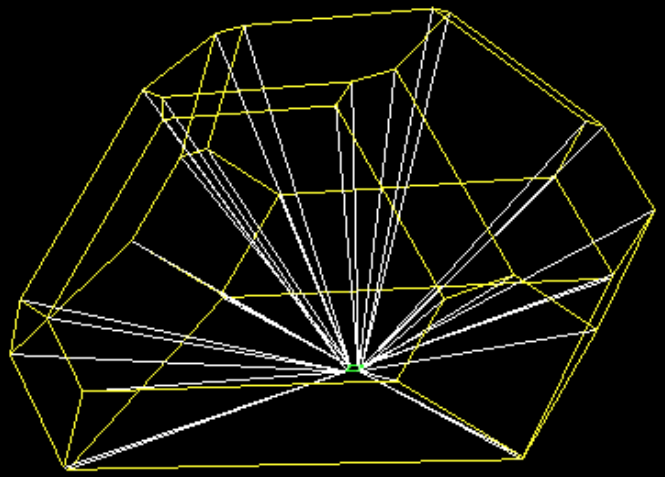

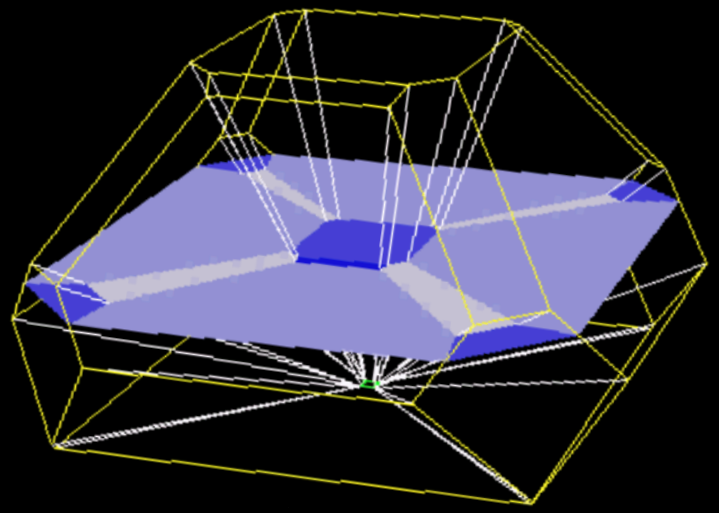

Above
Wireframe of growth sectors, schematic

Images from Growth program of the DTC

Below
Photo, UV Luminescence 1-3

top

middle

bottom

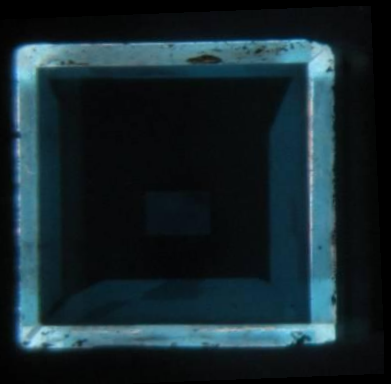

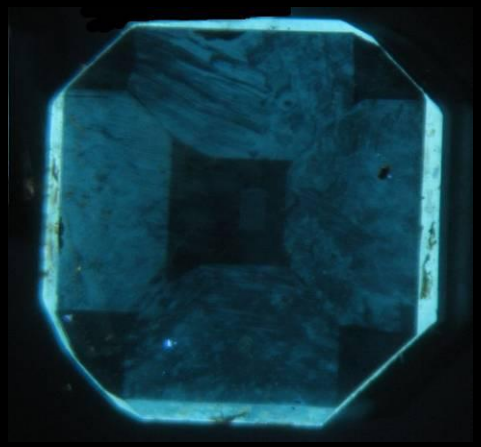

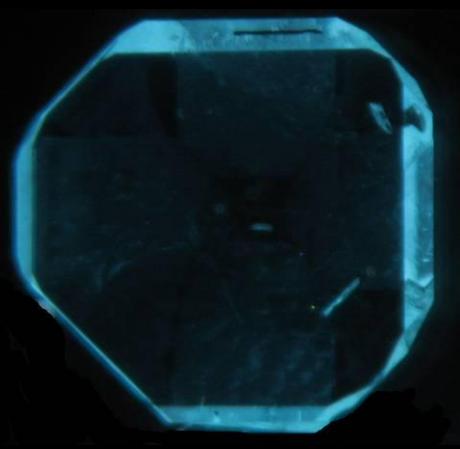

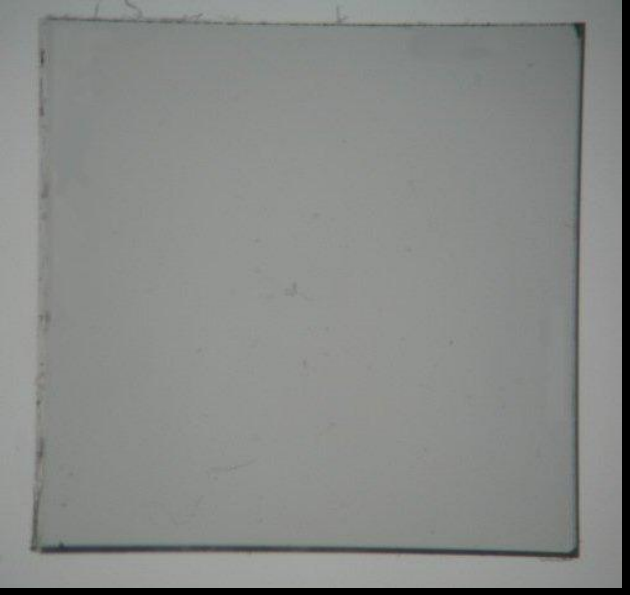

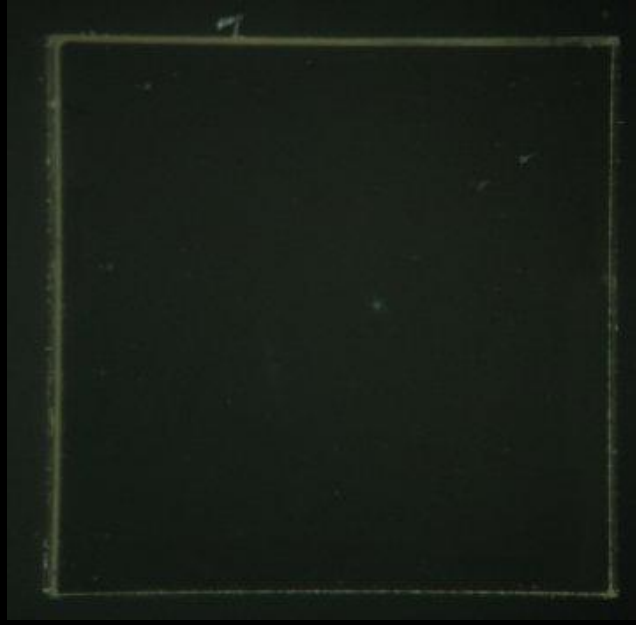

Clockwise

Visible image

Birefringence image

UV - luminescence

WB X-ray Topograph

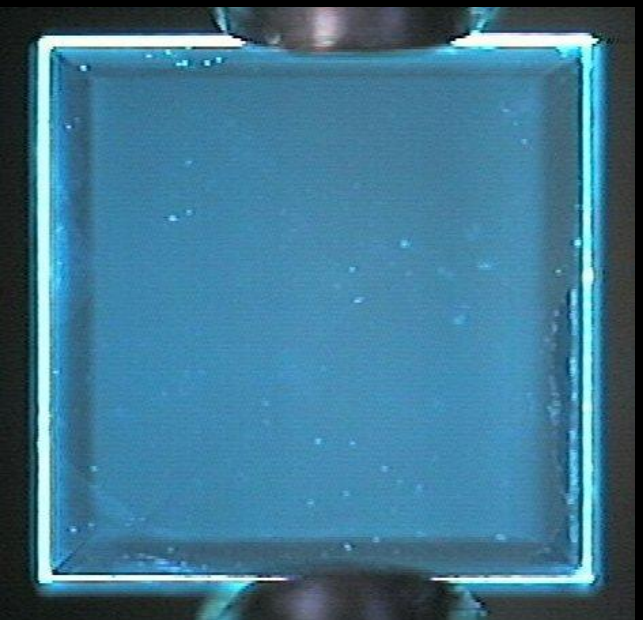

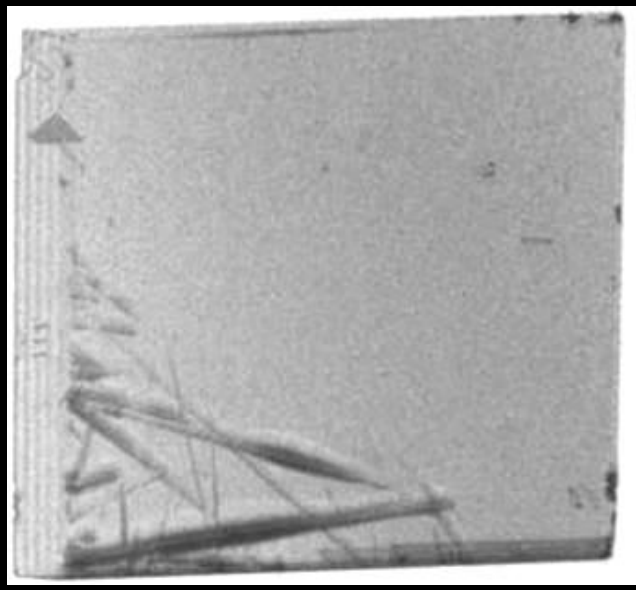

HPHT vs CVD

Techniques are complimentary – both are necessary

1. CVD growth conditions cold for diamond – allow better control of impurities however, defects can freeze in.
   Leads to purer diamond (c<1ppb), but residual strain is compromised (bundles of dislocations emanating from defects in substrate, maybe more still $\Delta\theta>10^{-6}$).
   Niche is Electronic Applications

2. HPHT growth conditions hotter, and in the pressure capsule its more difficult to control impurities, growth is in "annealing" conditions.
   Leads to low strain diamond $\Delta\theta\sim10^{-8}$, but more impurities, c<10ppb.
   Niche is Optical Applications

Situation evolves

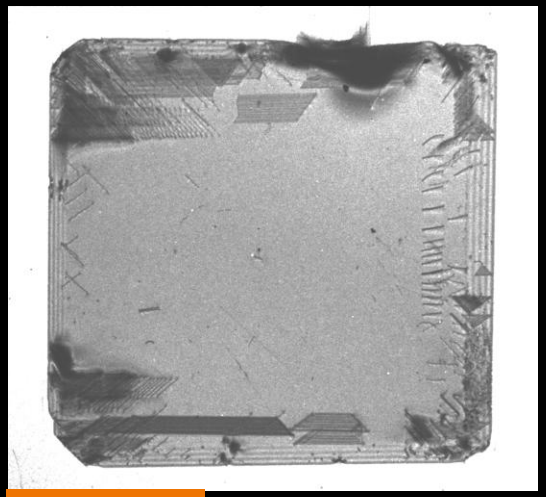

HPHT

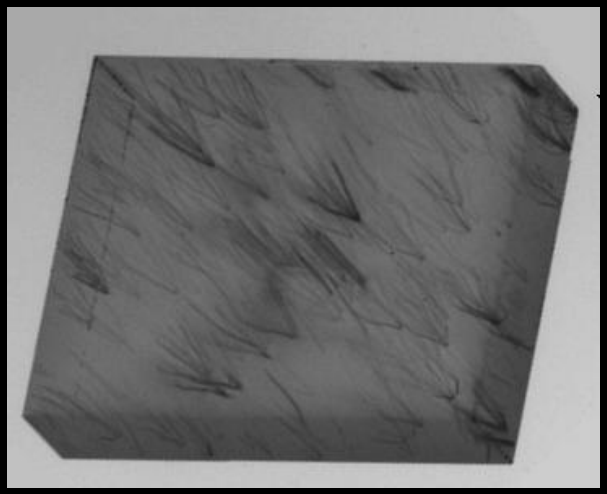

CVD

DRM17(2008)262

White Beam Topographs - In each case illustrative samples (not the best available)

High-resolution diffractometry set-up

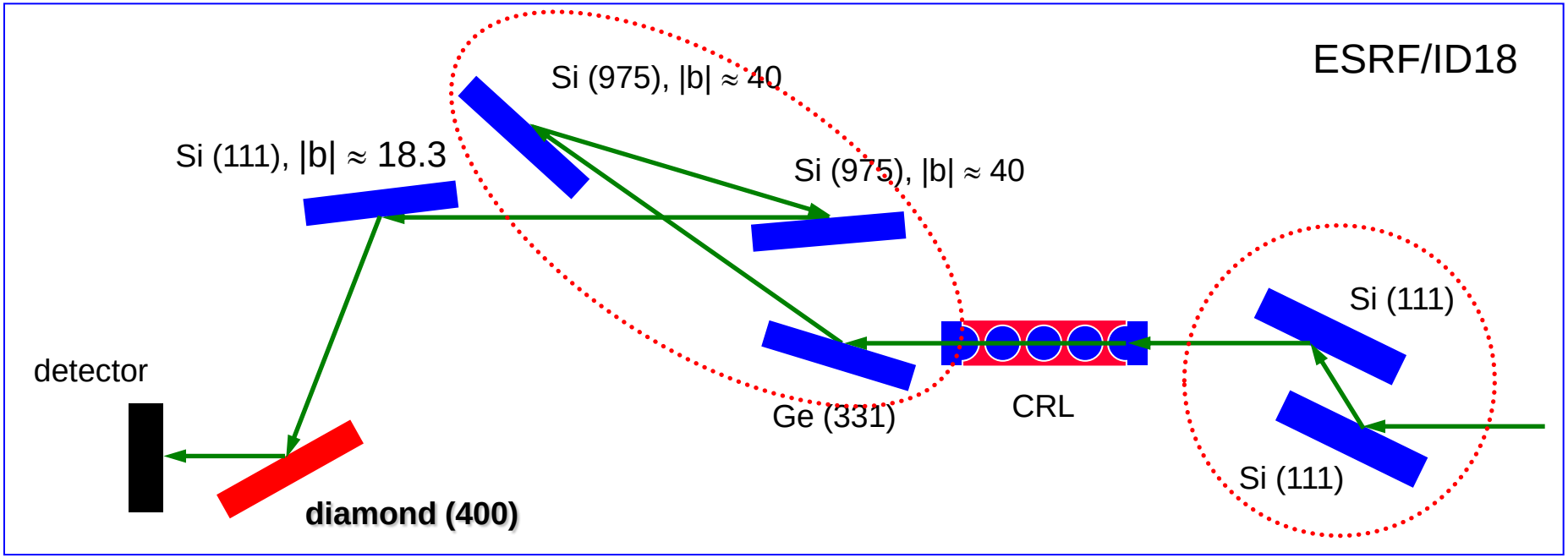

E = 14.413 keV

Δλ/λ ≈ 10^{-8} (≅ 0.0023”)

δθ ≈ 0.18”

WHITE BEAM TOPOGRAPHY and Rocking Curve Broadening

HPHT with inclusion

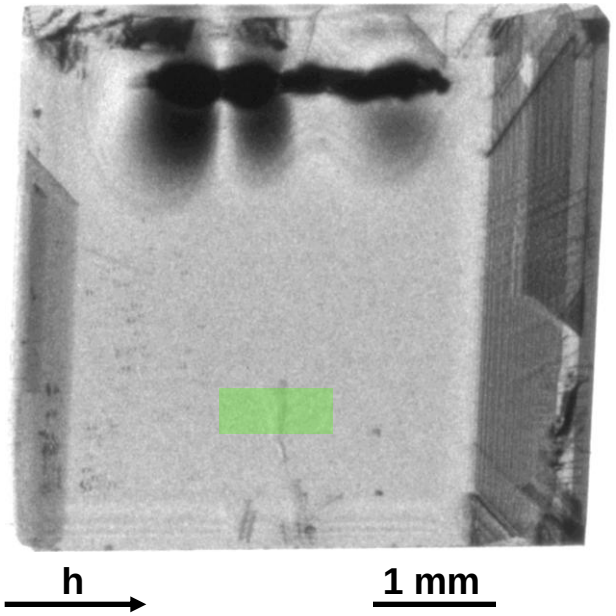

footprint = 1 x 0.4 mm

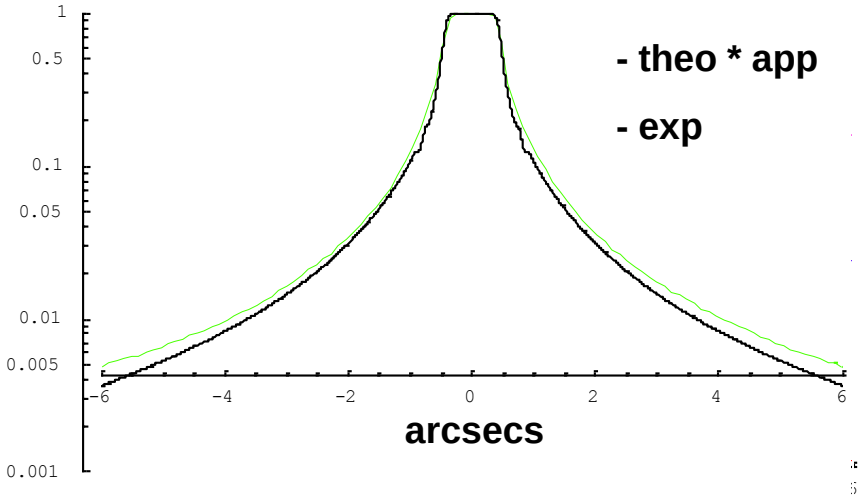

fit after convolution “defects broadening”

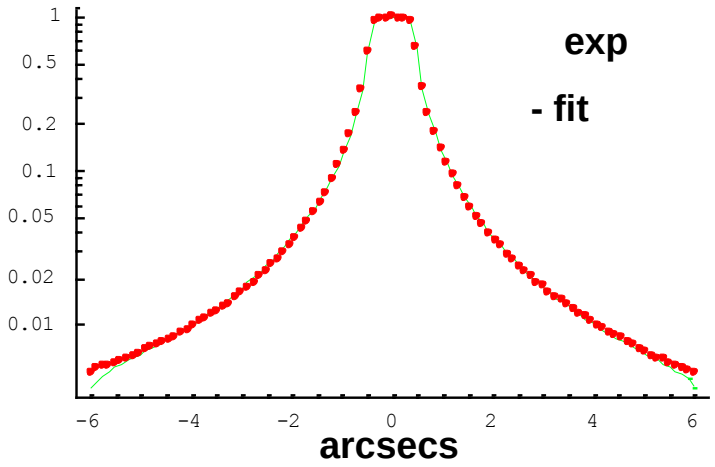

“defects broadening” function

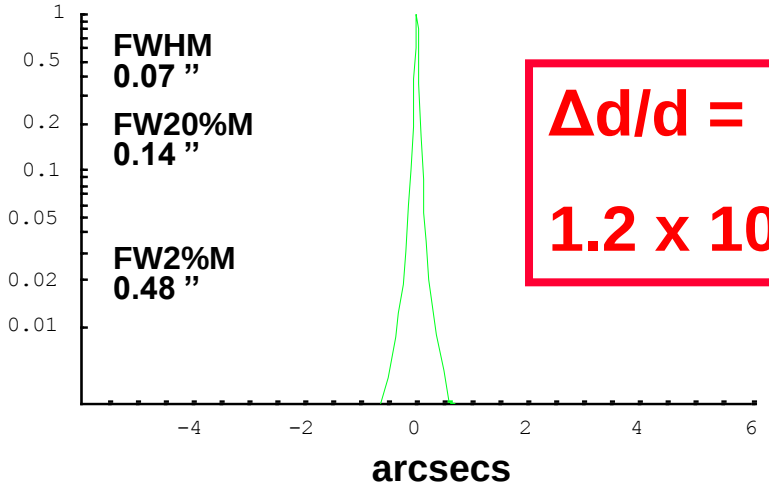

Δd/d =

1.2 x 10^{-5}

ESRF

Rocking Curve Imaging Principle

Wide, parallel X-ray beam
ID19 @ ESRF: 15 x 40 mm

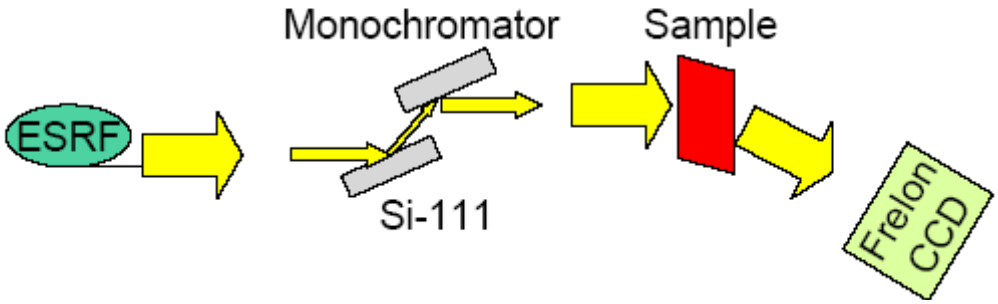

Series of topograms

3D block of Intensity data

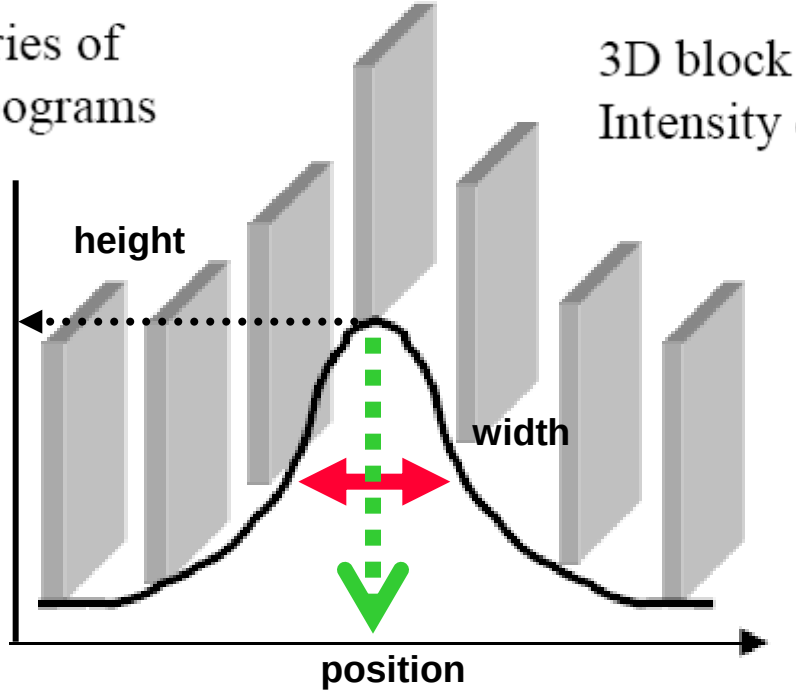

position

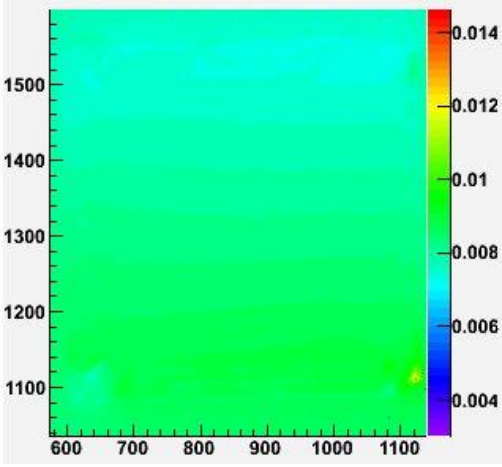

width

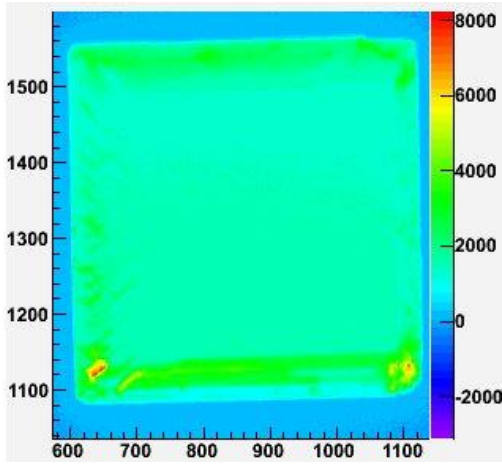

height

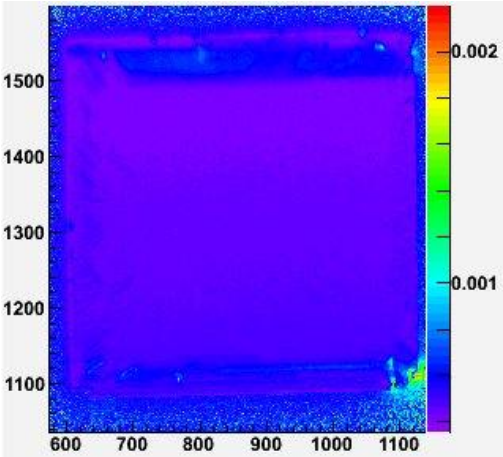

Bendable Monochromator

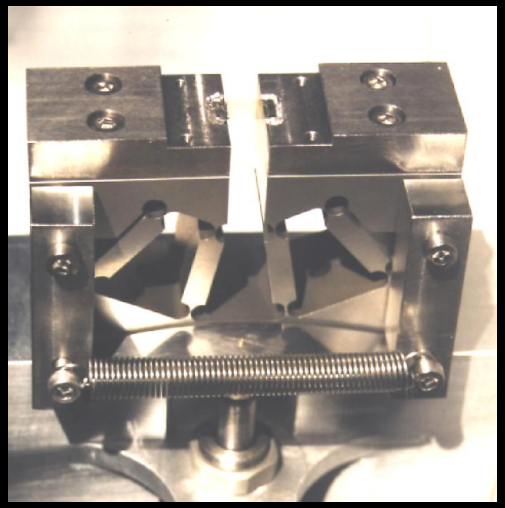

Micrometer scaled resolved X-ray diffraction image of diamond

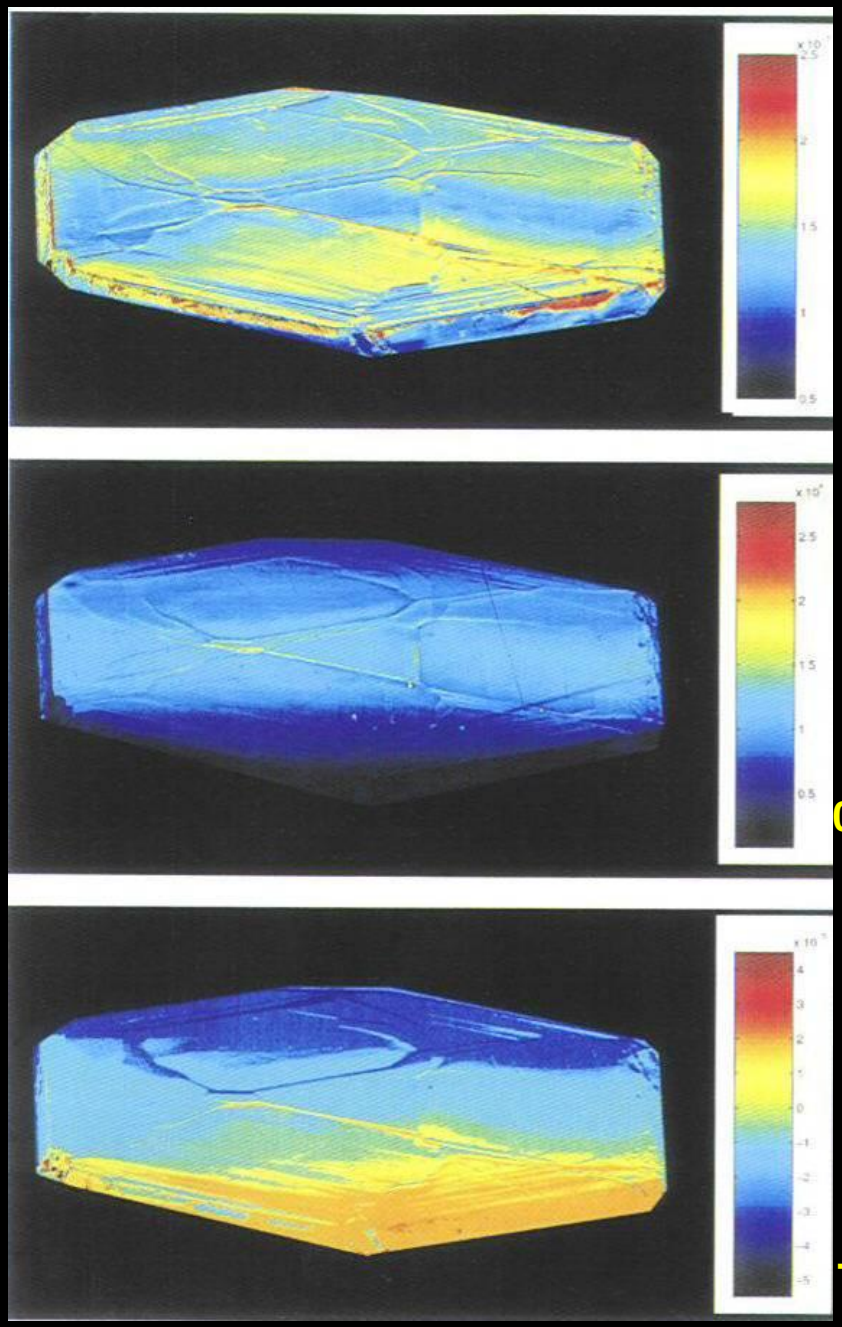

$$\delta\theta(\vec{r}) = \theta - \theta_B^{perf} - \tan\theta_B \frac{\Delta d}{d}(\vec{r}) \pm \Delta\varphi(\vec{r})$$

Quantification of strain at the 10^{-8} level

$$\delta\theta = \left.\frac{d\theta}{dR}\right|_{\theta_{wp}} \bullet \frac{\Delta I}{I_{max}}$$

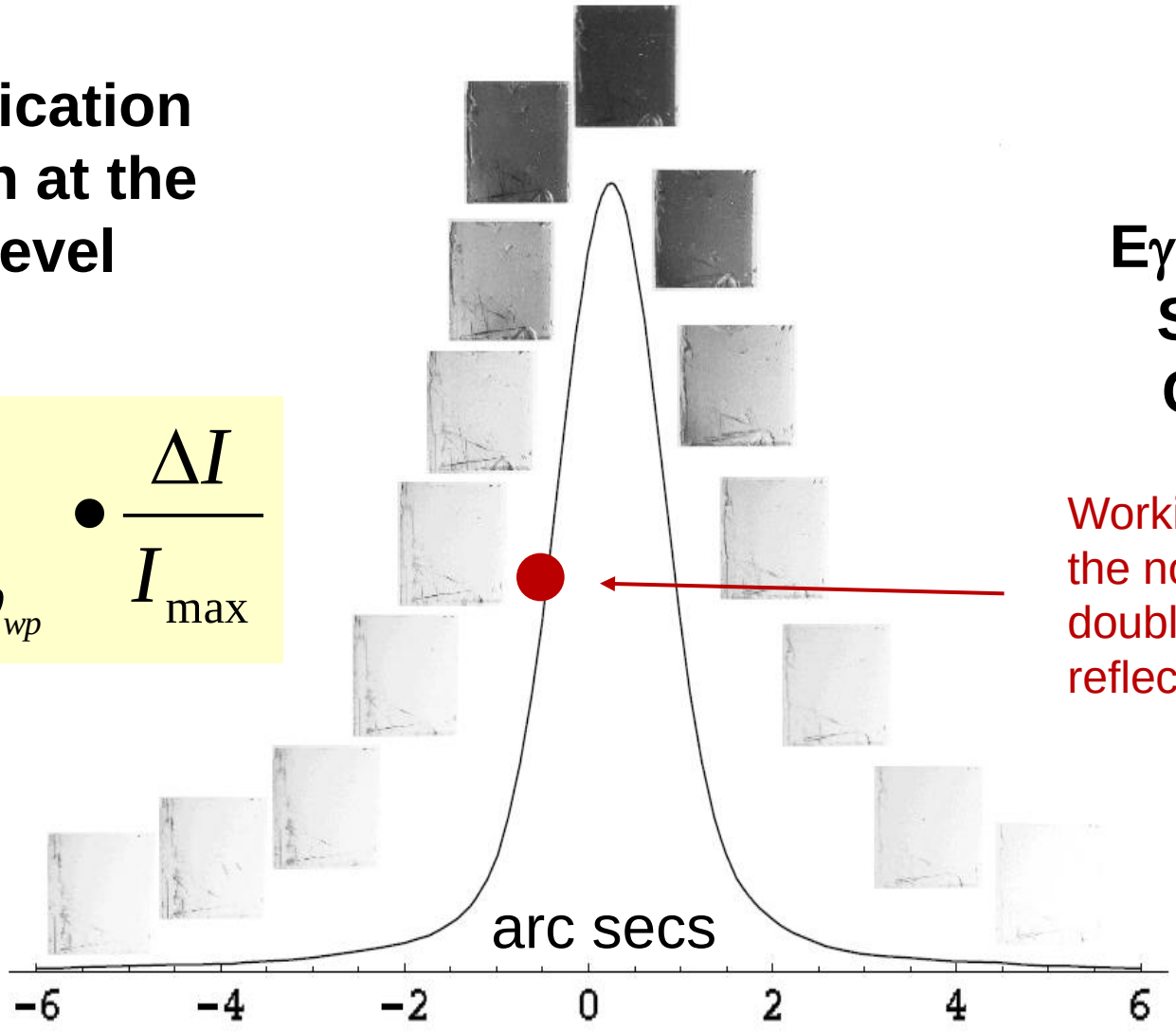

Eγ =12 keV
Si (444)
C* (115)

Working point on the non-dispersive double crystal reflectivity curve

Increasing strain sensitivity

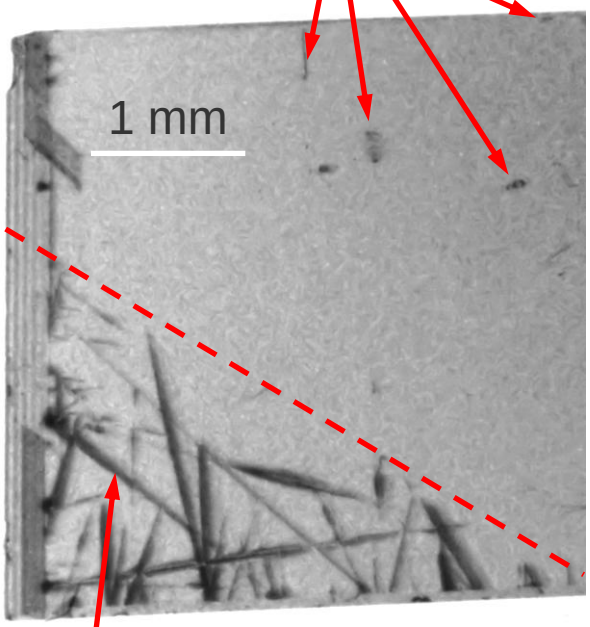

WBT
Laue case

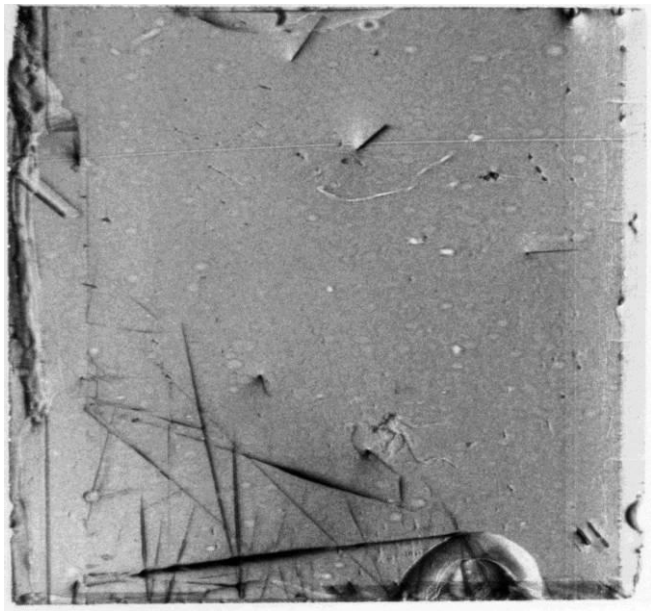

MPWT Bragg

12keV, Si [444] C^* [115]
$\Delta d/d > 4\ 10^{-8}$

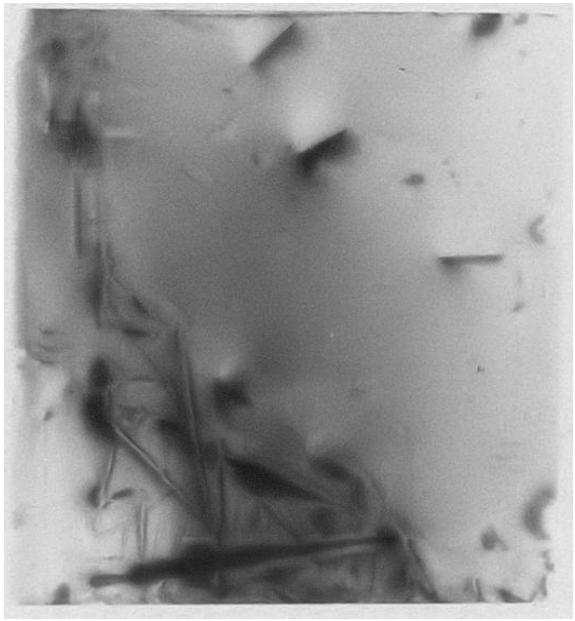

MPWT Bragg

20keV, Si [800] C^* [800]
$\Delta d/d > 1.2\ 10^{-8}$

Also with this **very high strain sensitivity**
a **rather homogenous zone** is present,
there crystal quality **close to that of silicon**

ESRF
Newsletter
45(2007))27

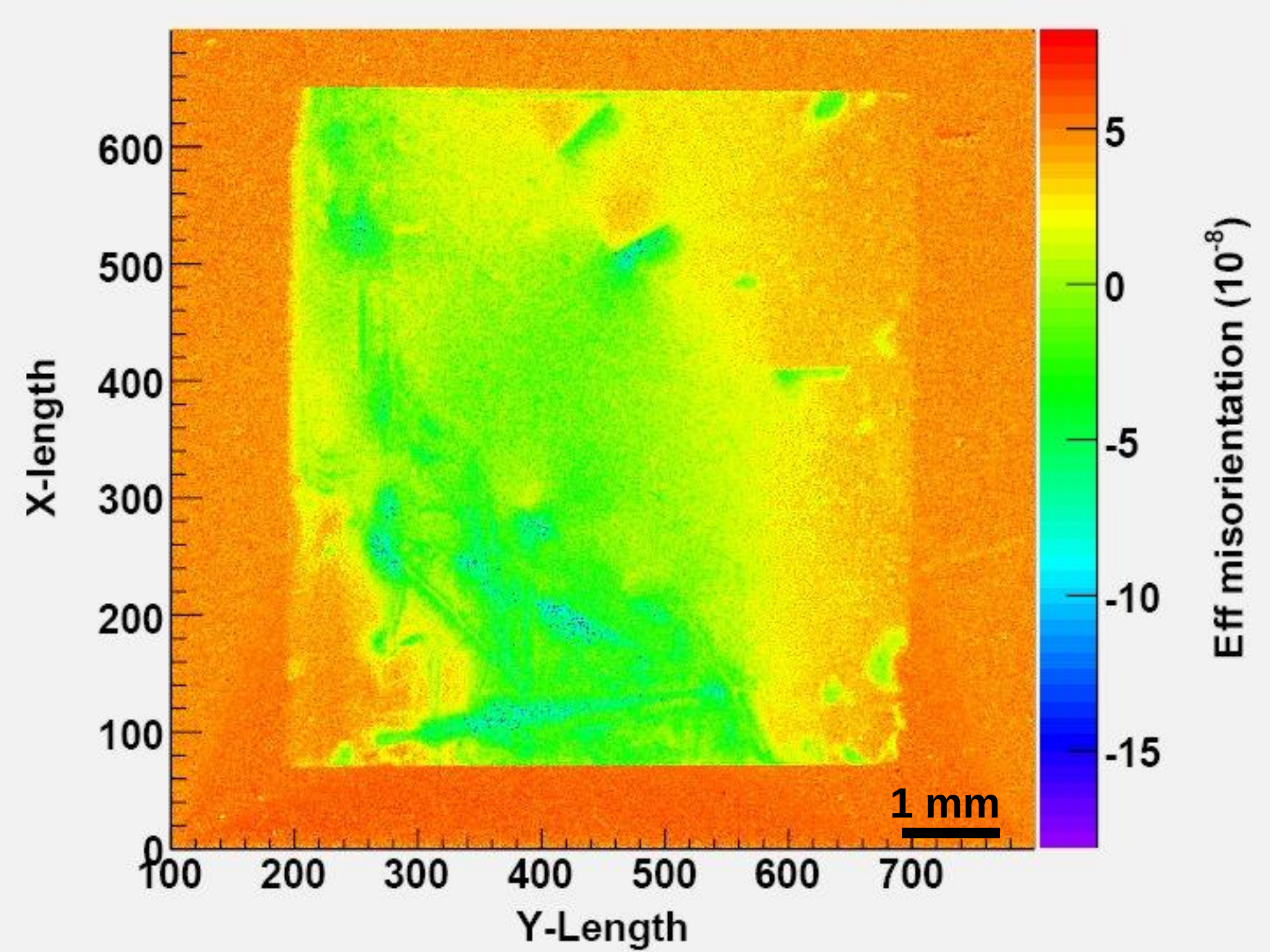
X-length
0
100
200
300
400
500
600
Y-Length
100
200
300
400
500
600
700
1 mm
Eff misorientation (10^{-8})
5
0
-5
-10
-15

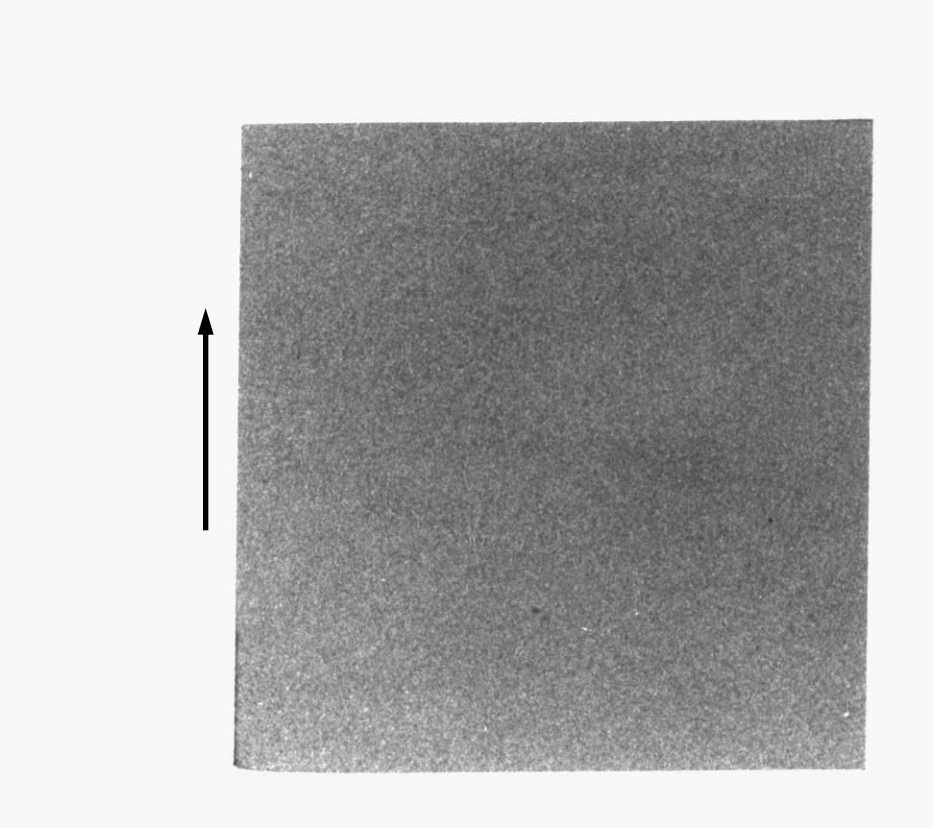

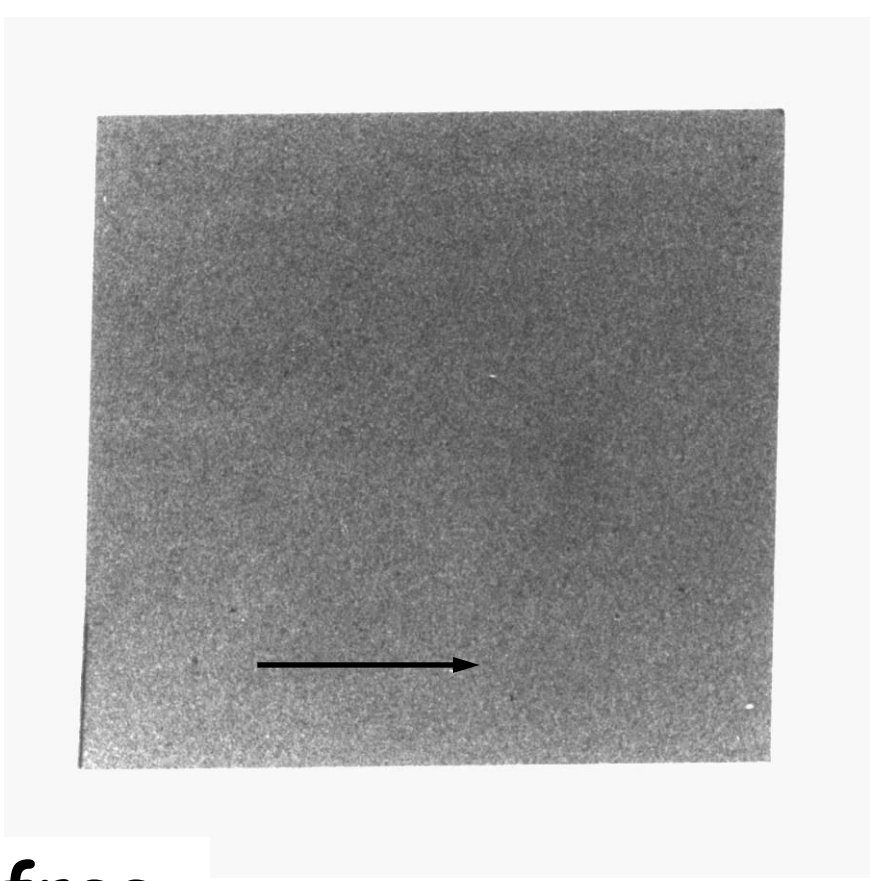

Dislocation free

-220 and 220-reflections

sample dimension 4x4 mm^2

The crystal quality seen with the strain sensitivity of white beam topography is very good! No macroscopic defects like dislocations are visible.

White beam topographs in transmission

ESRF

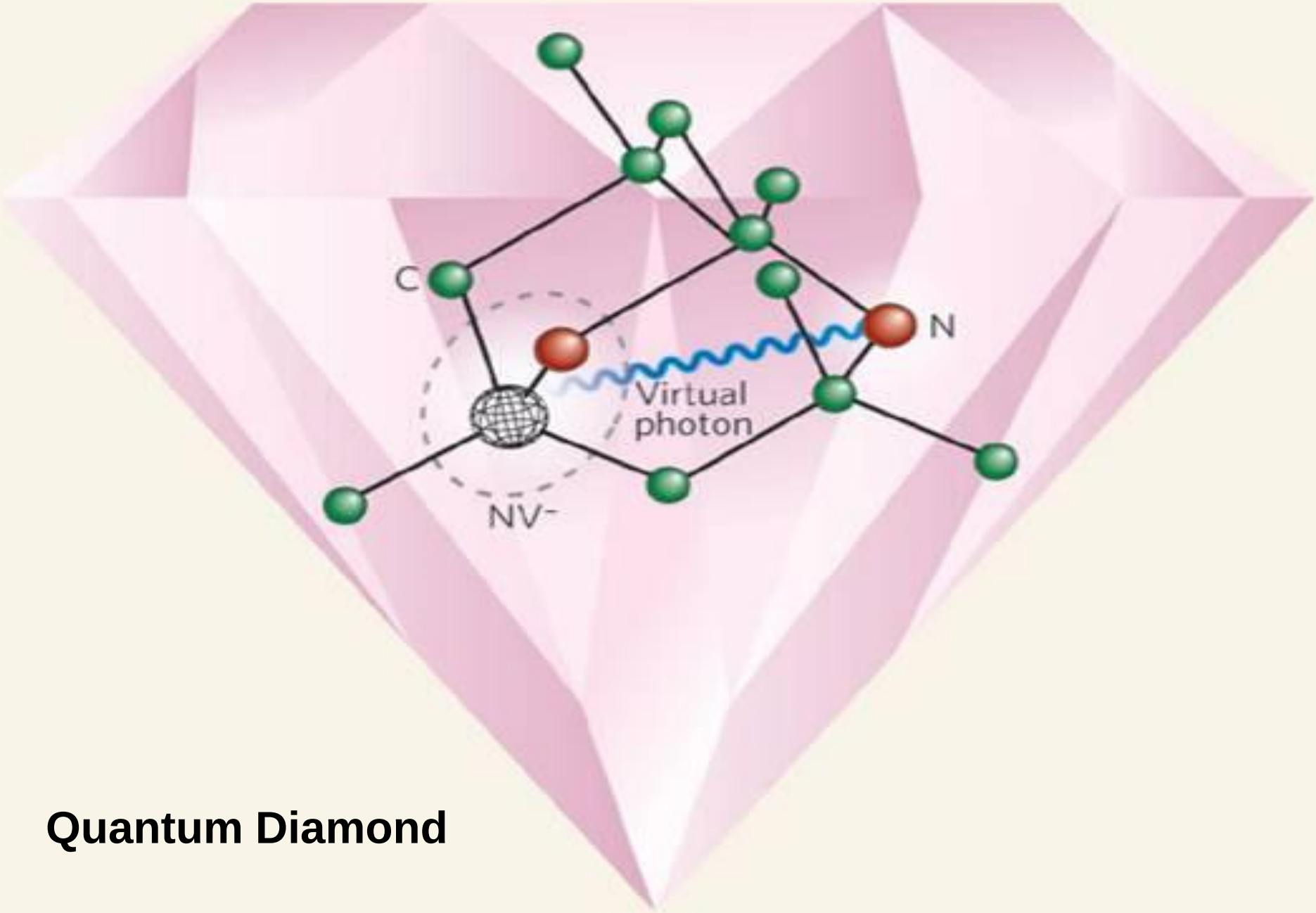

Quantum Diamond

Why study Muonium ?

1. Mu chemically similar to H
2. Dynamics are different
3. Reconcile Mu, H studies
4. Study quantum diffusion

	charge	spin	mass	moment	$\gamma / 2\pi$ (kHz G^{-1})	lifetime (μs)
e	$\pm$e	1/2	m_e = 0.51 MeV	657 μ_p	2800	∞
μ	$\pm$e	1/2	207 m_e = 105.7 MeV	3.18 μ_p	13.5	2.19
p	$\pm$e	1/2	1836 m_e = 938 MeV	μ_p	4.26	∞

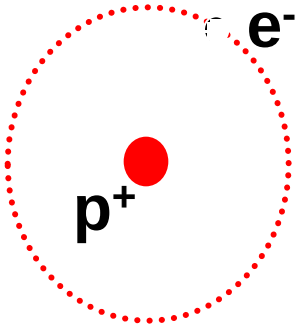

H		Mu
.999	m_r (m_e)	.995
.529	A_0 (A)	.531
-13.59	E_0 (eV)	-13.54
1.42	ω_0 (GHz)	4.46

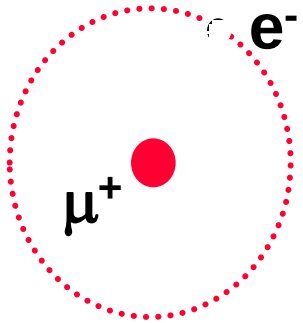

Focus on Hydrogen in diamond

Observations

- **Diamonds are always contaminated with H in some form**
- **Passivates acceptors and dopants**
- **Compensates deep recombination centres**
- **Possibly a mechanism to generate extended defects.**
- **H role in surface conductivity**
- **Possible role in shallowing of donor states – H_n-X complexes**
- **"MSR only unambiguous probe" – MA Stoneham in "The Properties of Diamond"**
- **Traps at the NV centre → NVH**

The search for shallow donors in diamond

Elemental :

- **N - E_d ~ 1700 meV, also deep**
- **P - E_d ~ 550 meV, μ_e ~ 200 cm^2/V, probably attracts defects**

Molecular :

Many theoretical suggestions

Bond compression shallows state

- **N-B-N**
- **N-H-N**
- **N-O**
- **H_n-X**

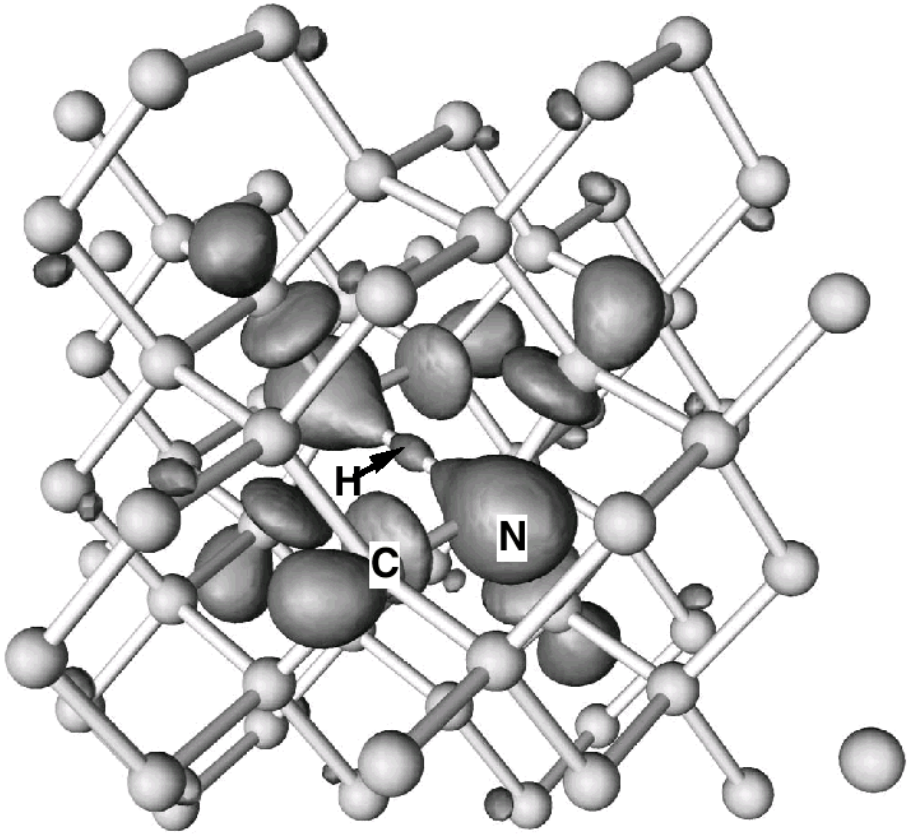

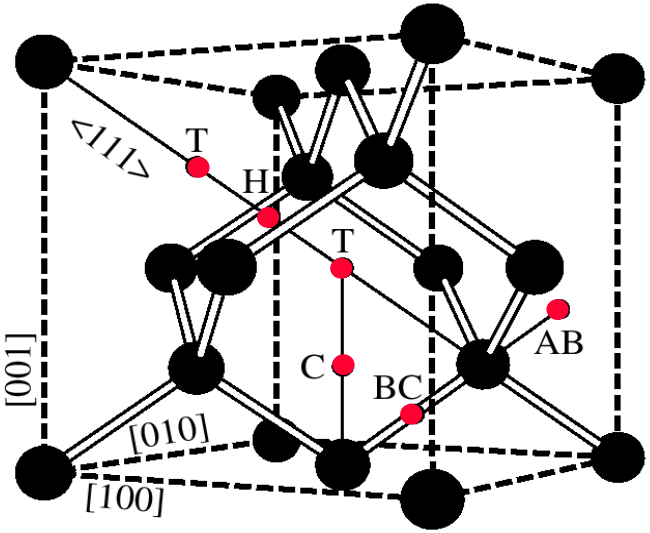

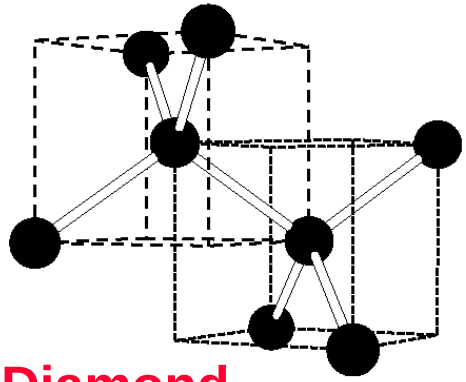

Diamond

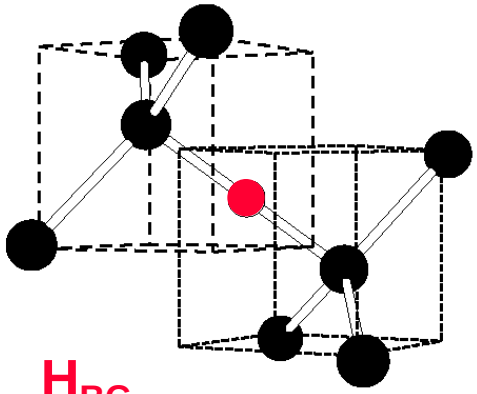

H_{BC}

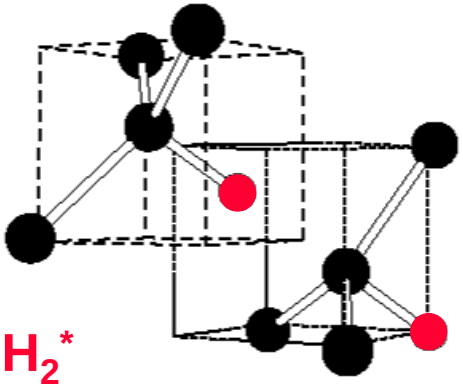

H_2^*

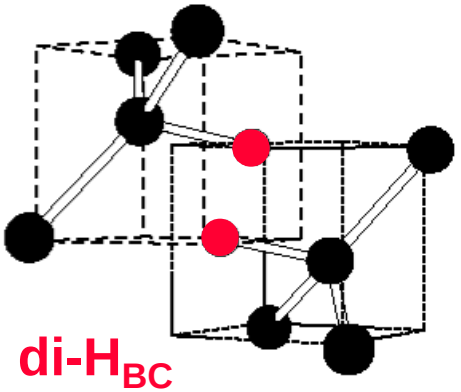

di-H_{BC}

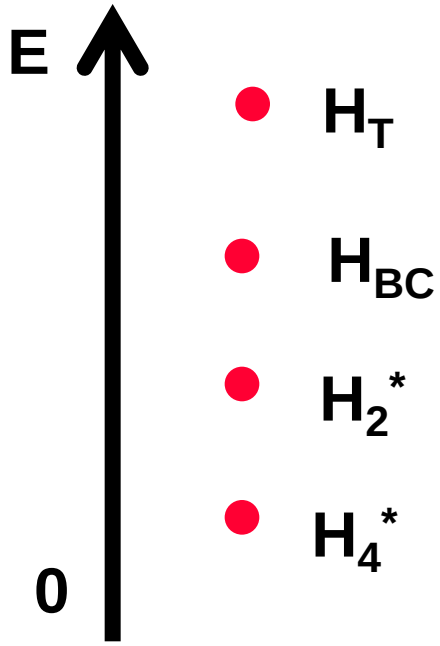

- H_T
- H_{BC}
- H_2^*
- H_4^*

Dislocation dipole

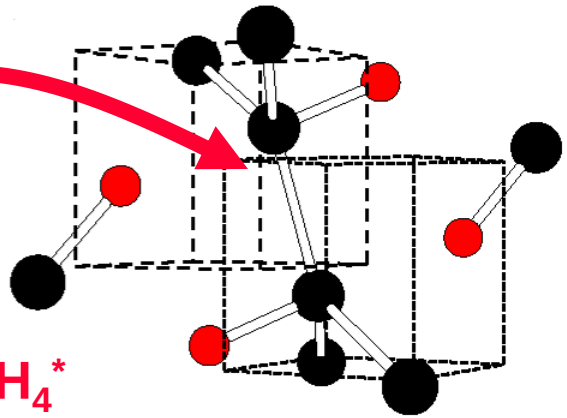

H_4^*

Typical MSR in Diamond

Diamond sample	$F_{MuT}(\%)$	$F_{MuBC}(\%)$	$F_d(\%)$	$F_{MuX}(\%)$	MF(%)
HPHT IIa SC C_N ~ 10 ppb	54 ± 2	30 ± 1	4 ± 1		12 ± 4
CVD PC C_N ~ 1 ppm	50.2	6.8	19.4		23.6
CVD PC C_N ~ 1 ppm	50	-	6		-
IIa SC C_N ~ 1 ppm	68.9	22.7	8.1		0.3
IIa SC C_N ~ 1 ppm	65	25	10		0
Ia C_N ~ 100 ppm	30	0	10	60	

TF MSR for Tetrahedral Muonium - Mu_T

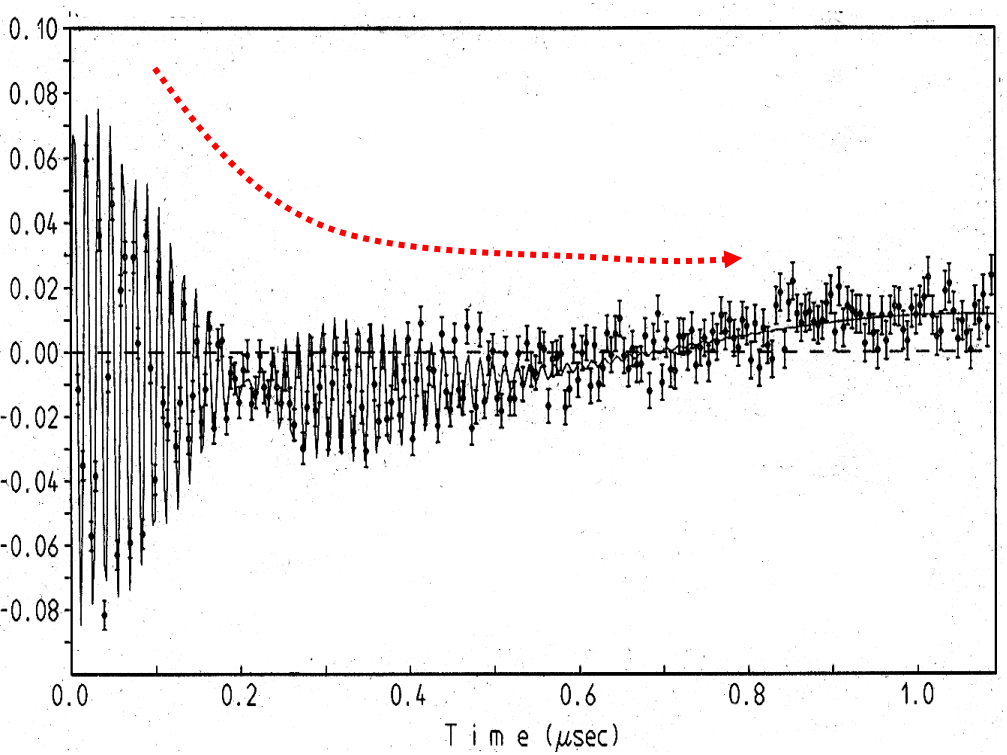

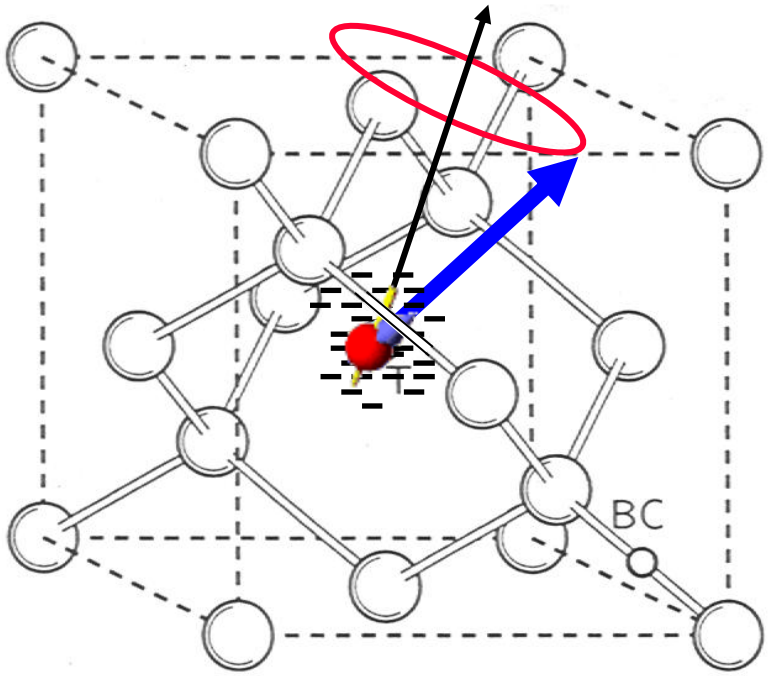

Beating of the two closely spaced precession frequencies ν_{12} and ν_{23}
Note the damping of the oscillations

Extract the depolarisation rate $\lambda(T)$

Four measurements of the Muonium Diffusion

1. **TF Methods**
   a. **Ensemble dephases by different arrival times at traps.**
      - **Boron Impurities**
      - **Vacancies**
   b. **Ensemble dephases due to motion against a background of randomly oriented moments**
      - **^{13}C enriched diamond**
2. **LF Methods**
   a. **Depolarisation by spin-lattice relaxation**
      - **^{13}C enriched diamond**

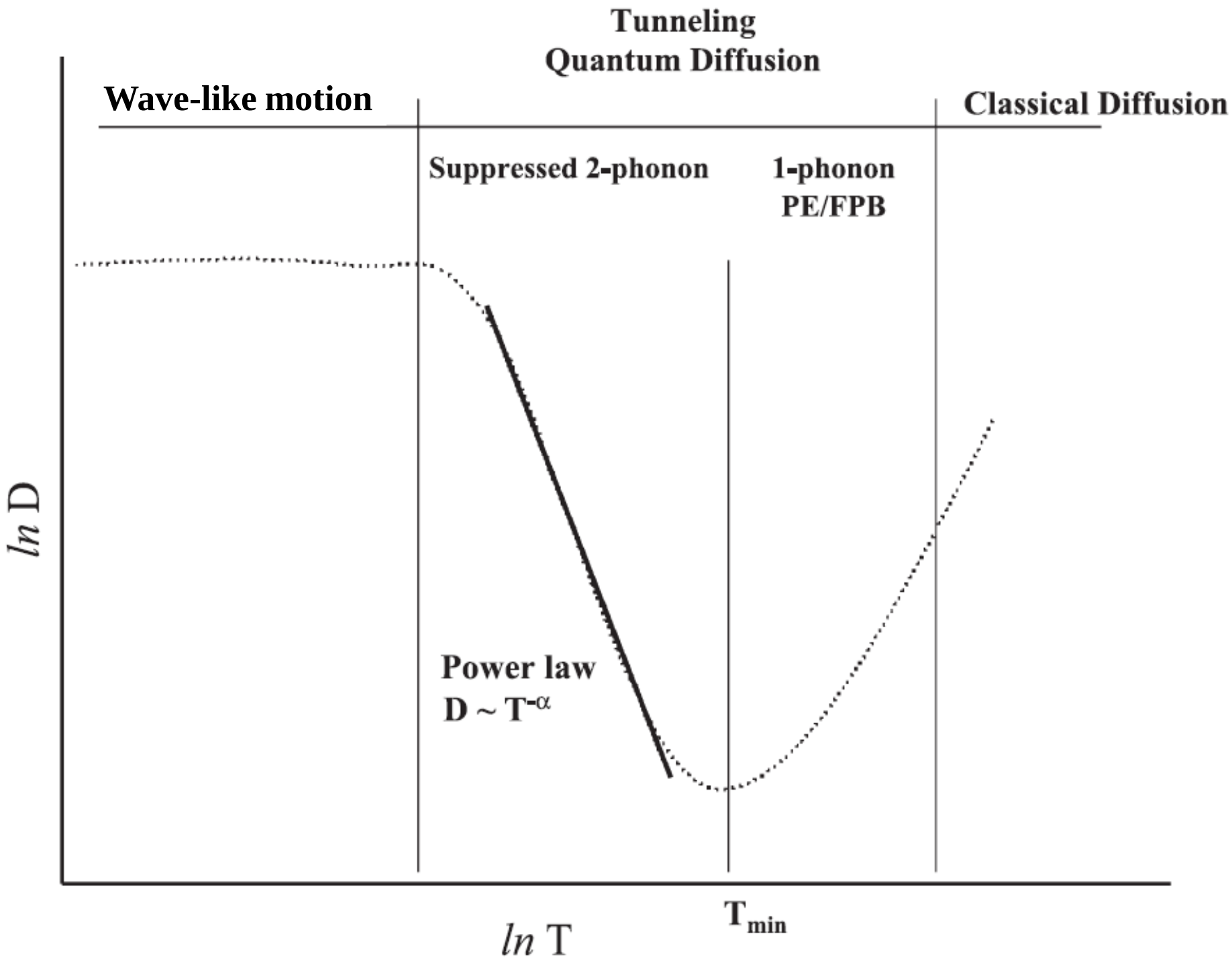
Tunneling
Quantum Diffusion
Wave-like motion
Classical Diffusion
Suppressed 2-phonon
1-phonon
PE/FPB
Power law
D ~ T-α
ln D
ln T
Tmin

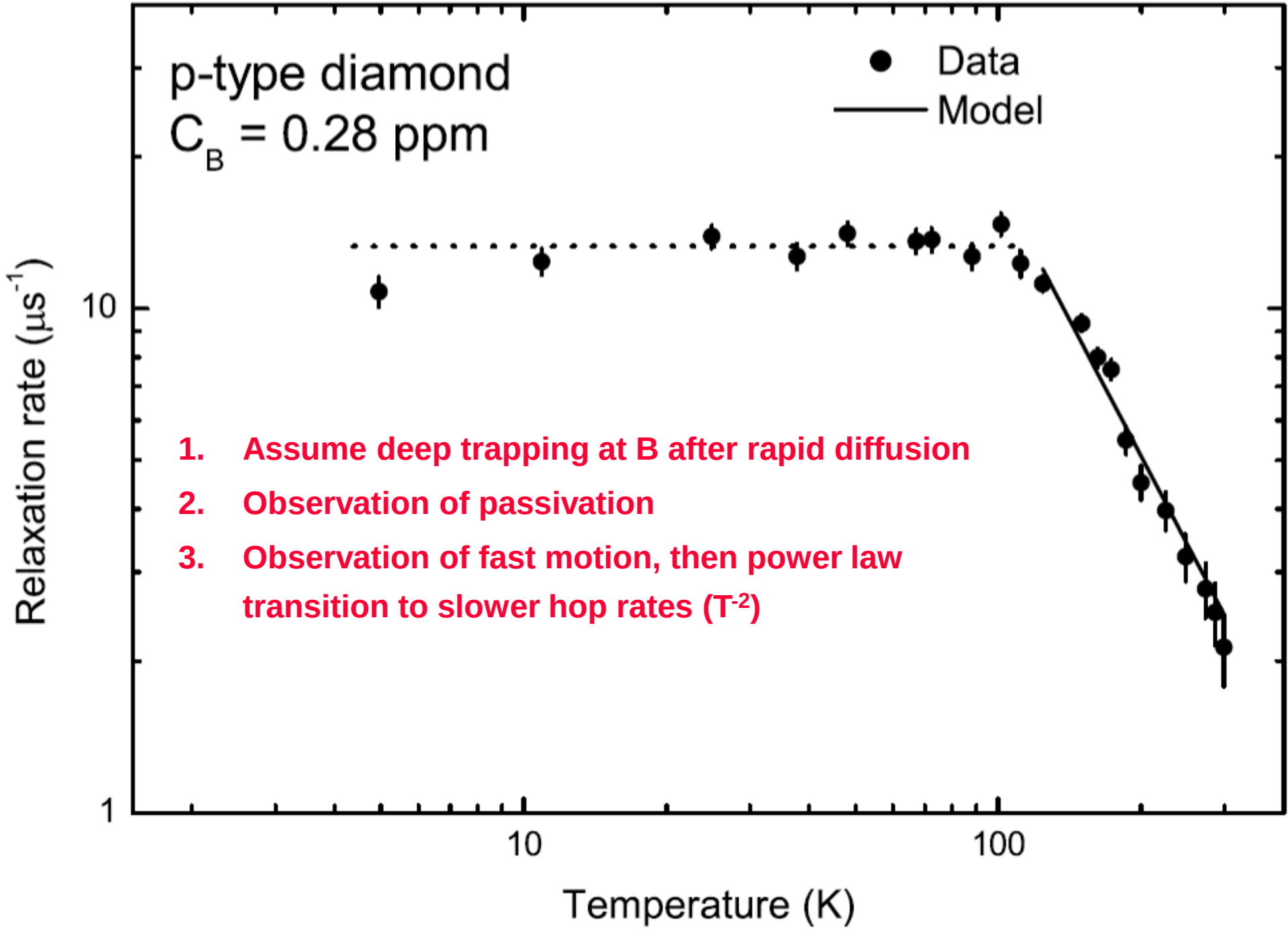
p-type diamond
C_B = 0.28 ppm
Data
Model
1. Assume deep trapping at B after rapid diffusion
2. Observation of passivation
3. Observation of fast motion, then power law transition to slower hop rates (T^{-2})
Relaxation rate (μs^{-1})
10
1
10
100
Temperature (K)

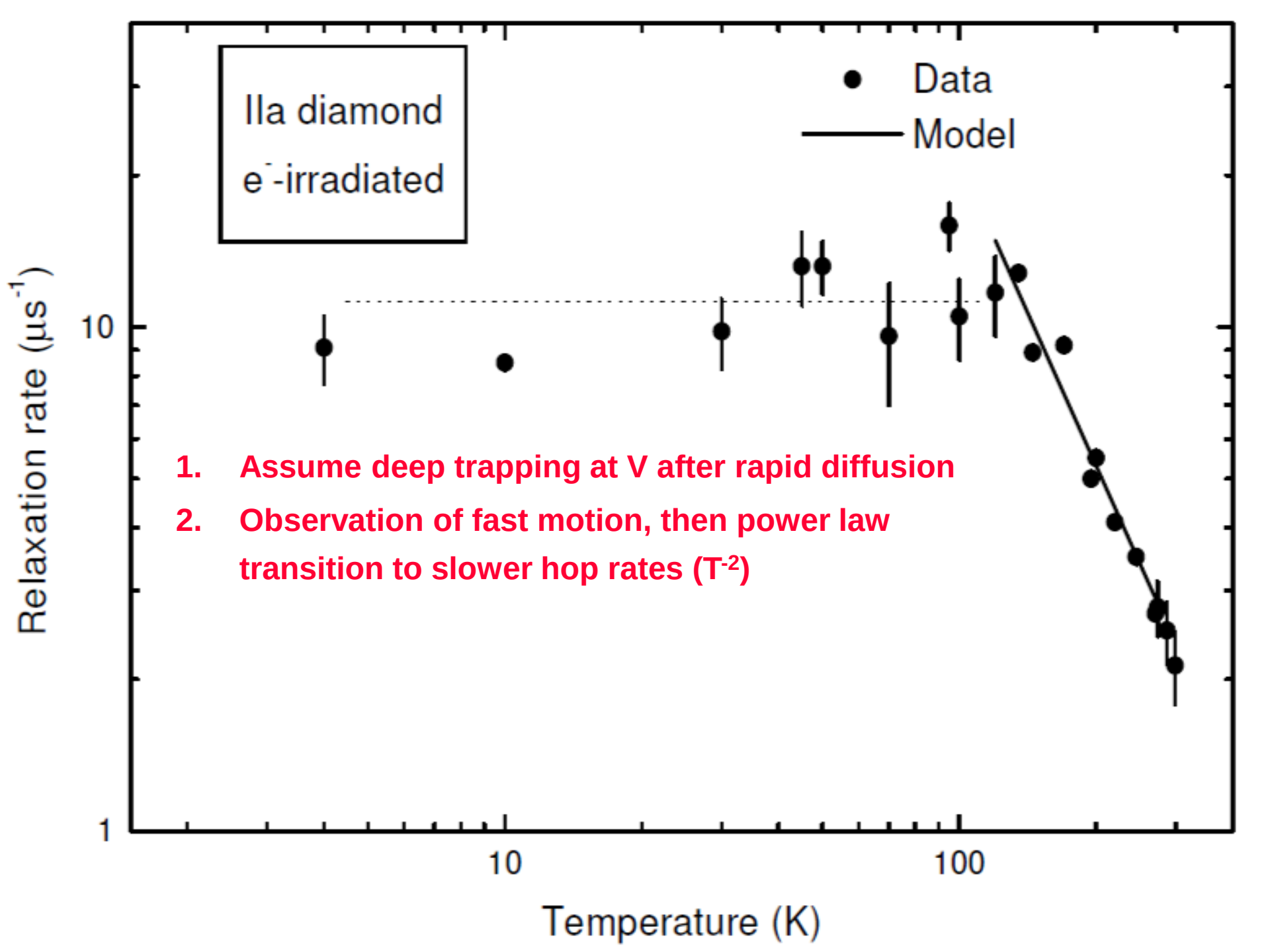
IIa diamond
e⁻-irradiated
Data
Model
Relaxation rate (μs⁻¹)
10
1
10
100
Temperature (K)
1. Assume deep trapping at V after rapid diffusion
2. Observation of fast motion, then power law transition to slower hop rates (T⁻²)

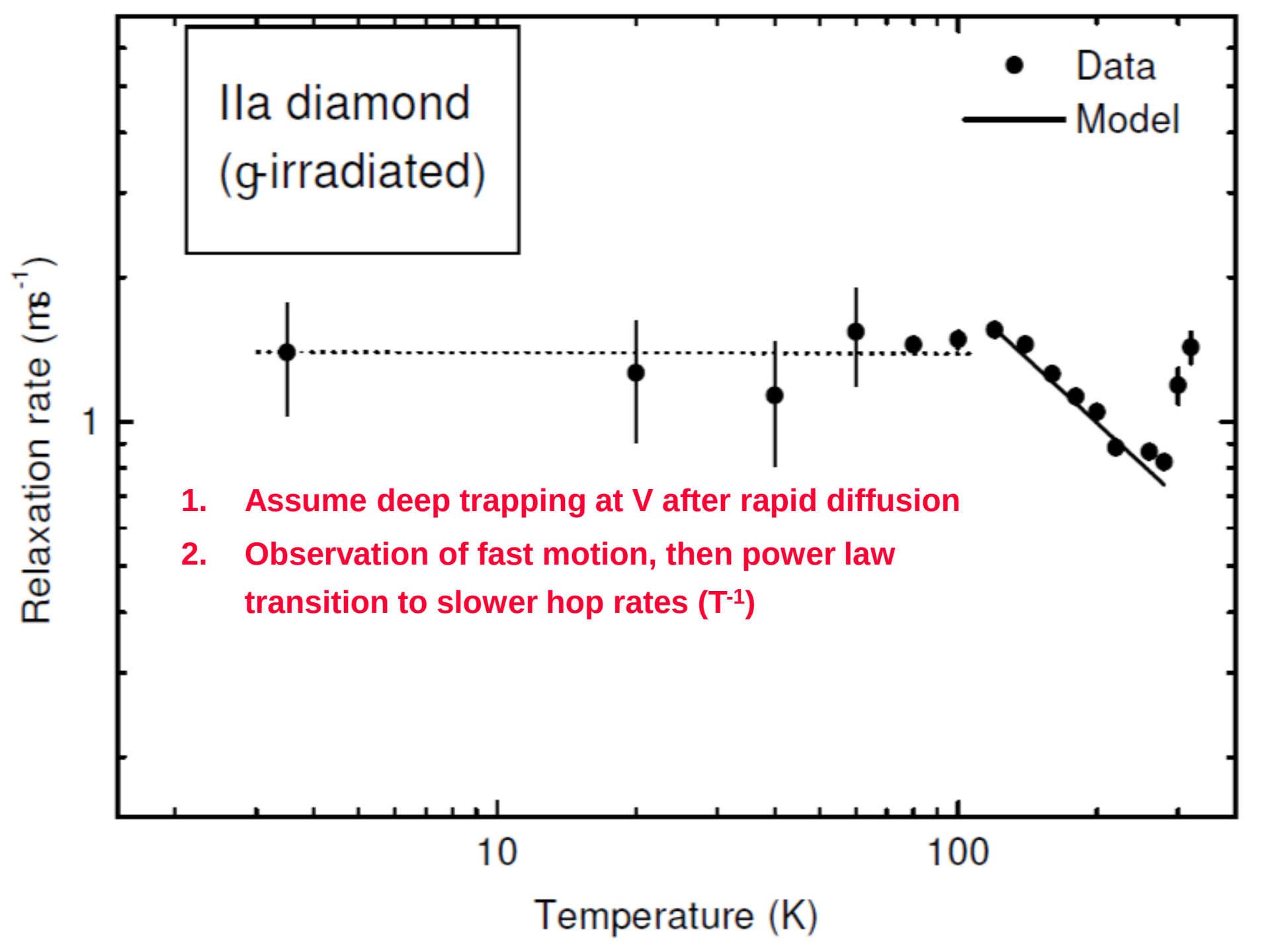

1. **Assume deep trapping at V after rapid diffusion**
2. **Observation of fast motion, then power law transition to slower hop rates (T^{-1})**

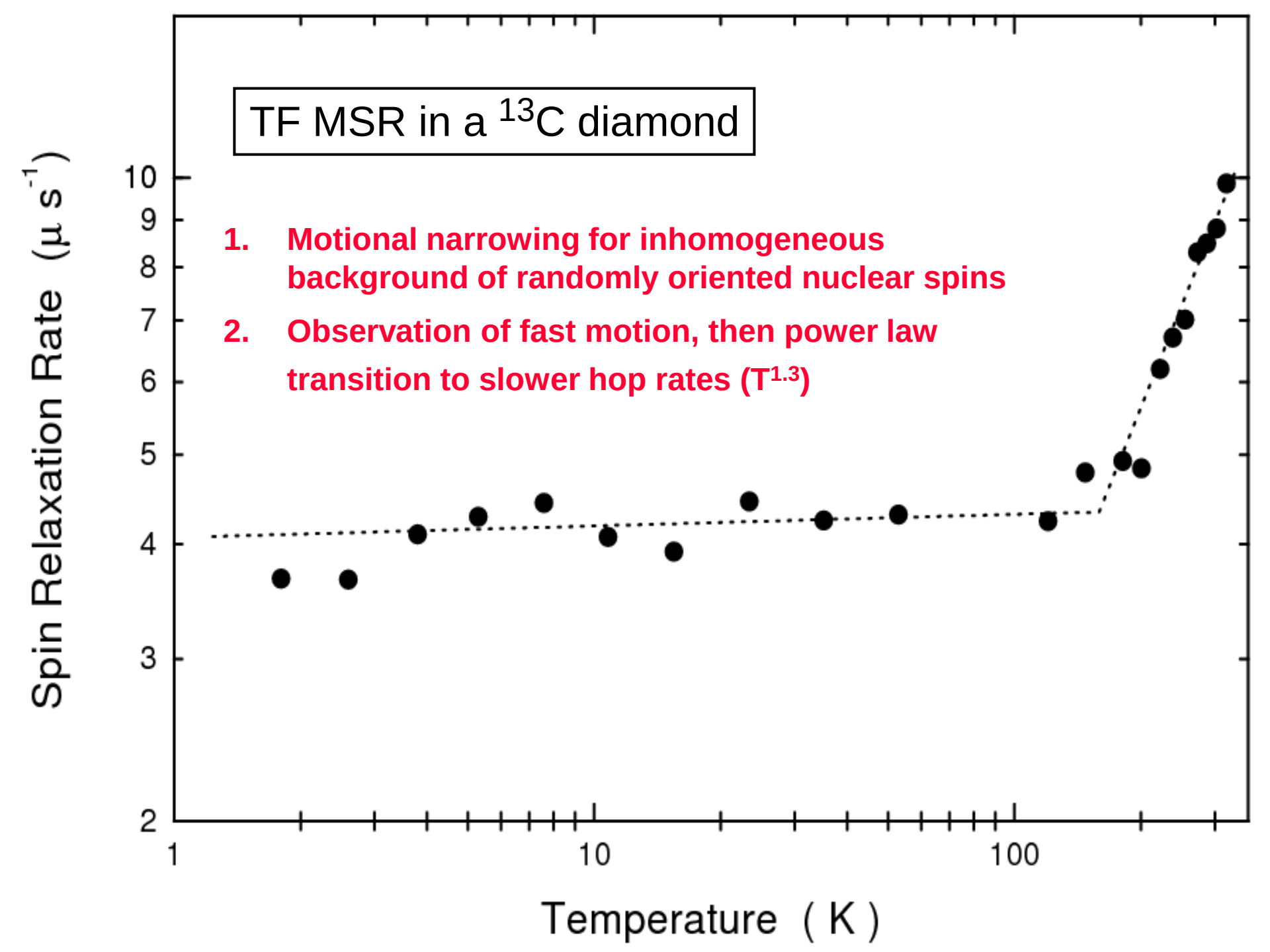
TF MSR in a ^{13}C diamond
1. Motional narrowing for inhomogeneous background of randomly oriented nuclear spins
2. Observation of fast motion, then power law transition to slower hop rates ($T^{1.3}$)
Spin Relaxation Rate (μs^{-1})
10
9
8
7
6
5
4
3
2
1
10
100
Temperature (K)

LF MSR in a ^{13}C diamond

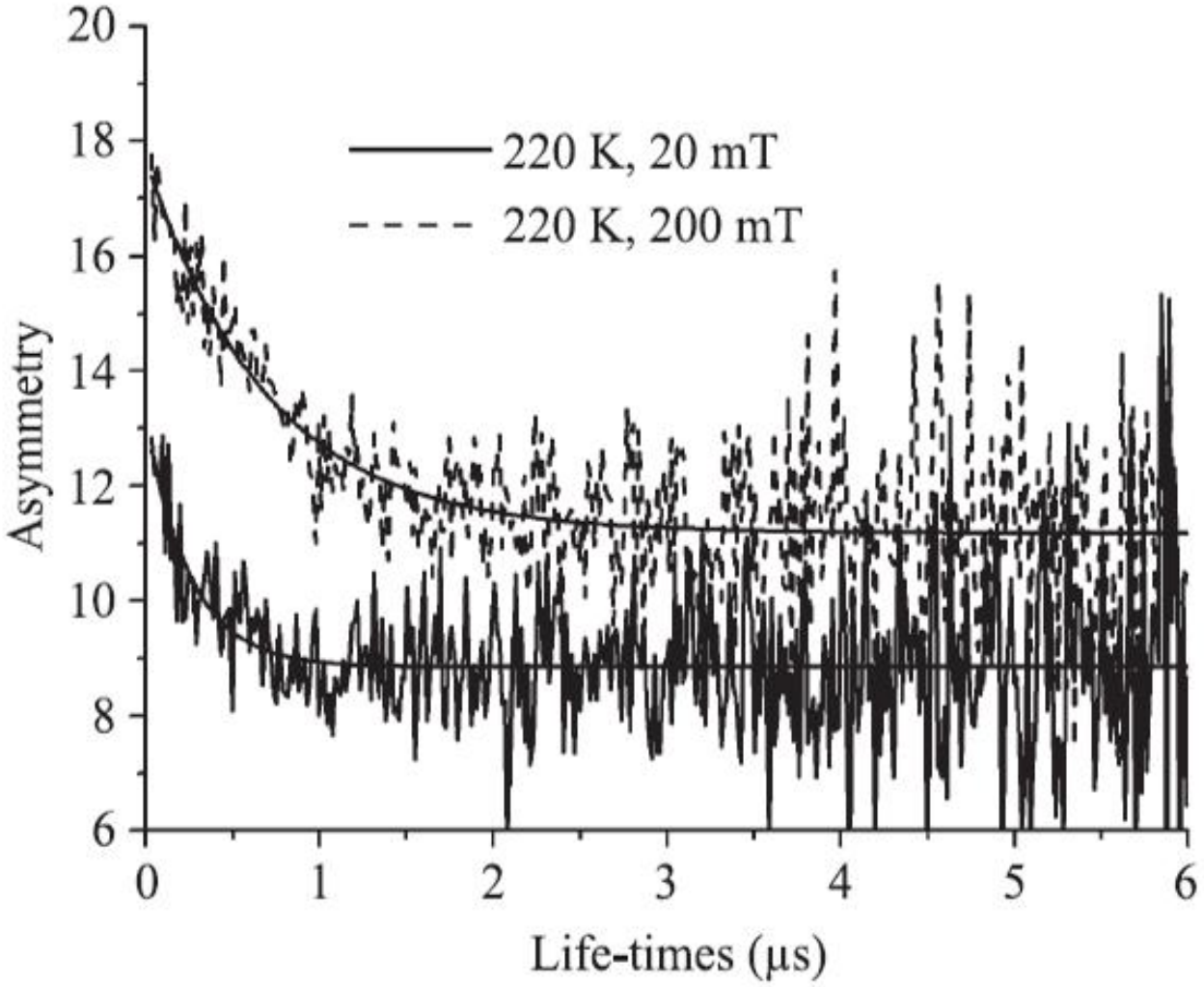

Longitudinal field muon decay spectra obtained in ^{13}C diamond at the temperature of 220 K and the applied magnetic fields of 20 and 200 mT.

LF MSR in a ^{13}C diamond

Data Analysis by Redfield Method

$$P_Z(t) = \exp(-t/T_1(B,T)) + C$$

$$T_1^{-1} \approx \left(1 - x/\sqrt{1+x^2}\right) \frac{\delta_{ex}^2 \tau_c}{1 + \omega_{12}^2 \tau_c^2}$$

$$\omega_{12} = \frac{\omega_0}{2}\left(1 + x\Gamma_-/\Gamma_+ - \sqrt{1+x^2}\right)$$

$$\Gamma_{\pm} = (g_e \mu_B \pm g_\mu \mu_\mu)(2\hbar)$$

$$x = 2\Gamma_+ B/\omega_0$$

Fit this expression to all Time Differential LF spectra at all temperatures simultaneously, and extract the **nuclear hyperfine constant** and **hop rate**.

LF MSR in a ^{13}C diamond

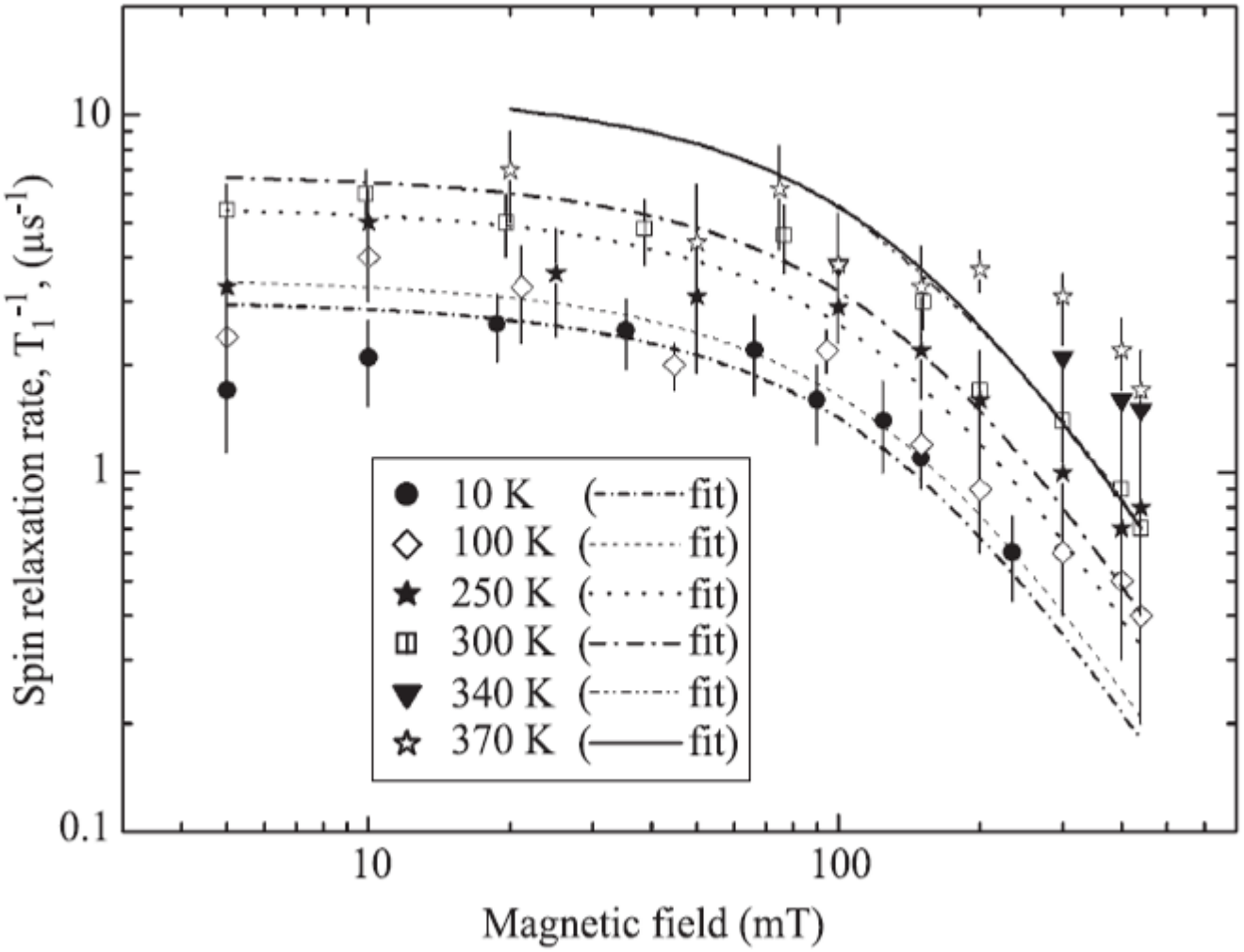

LF MSR in a ^{13}C diamond

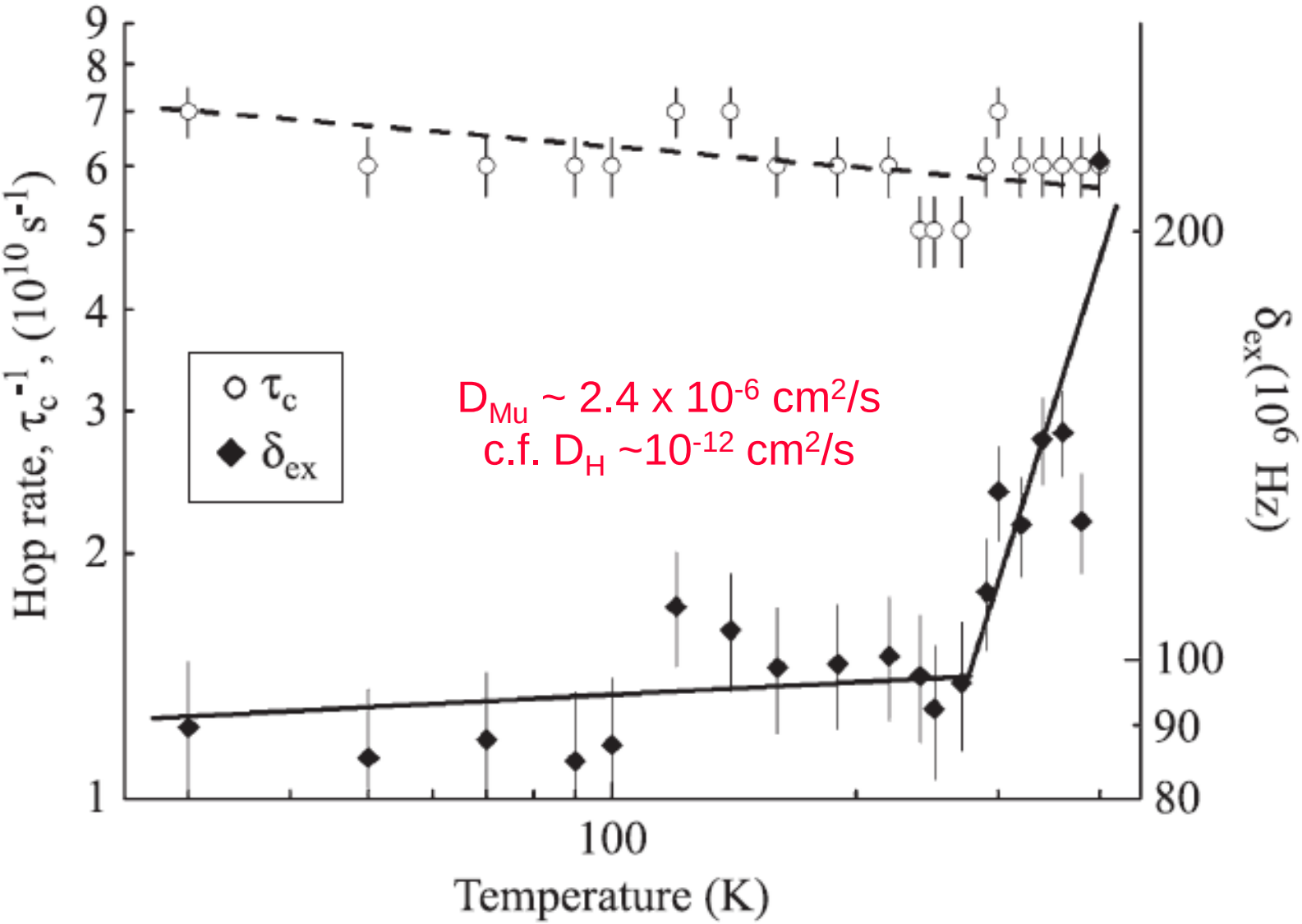

LF MSR in a ^{13}C diamond

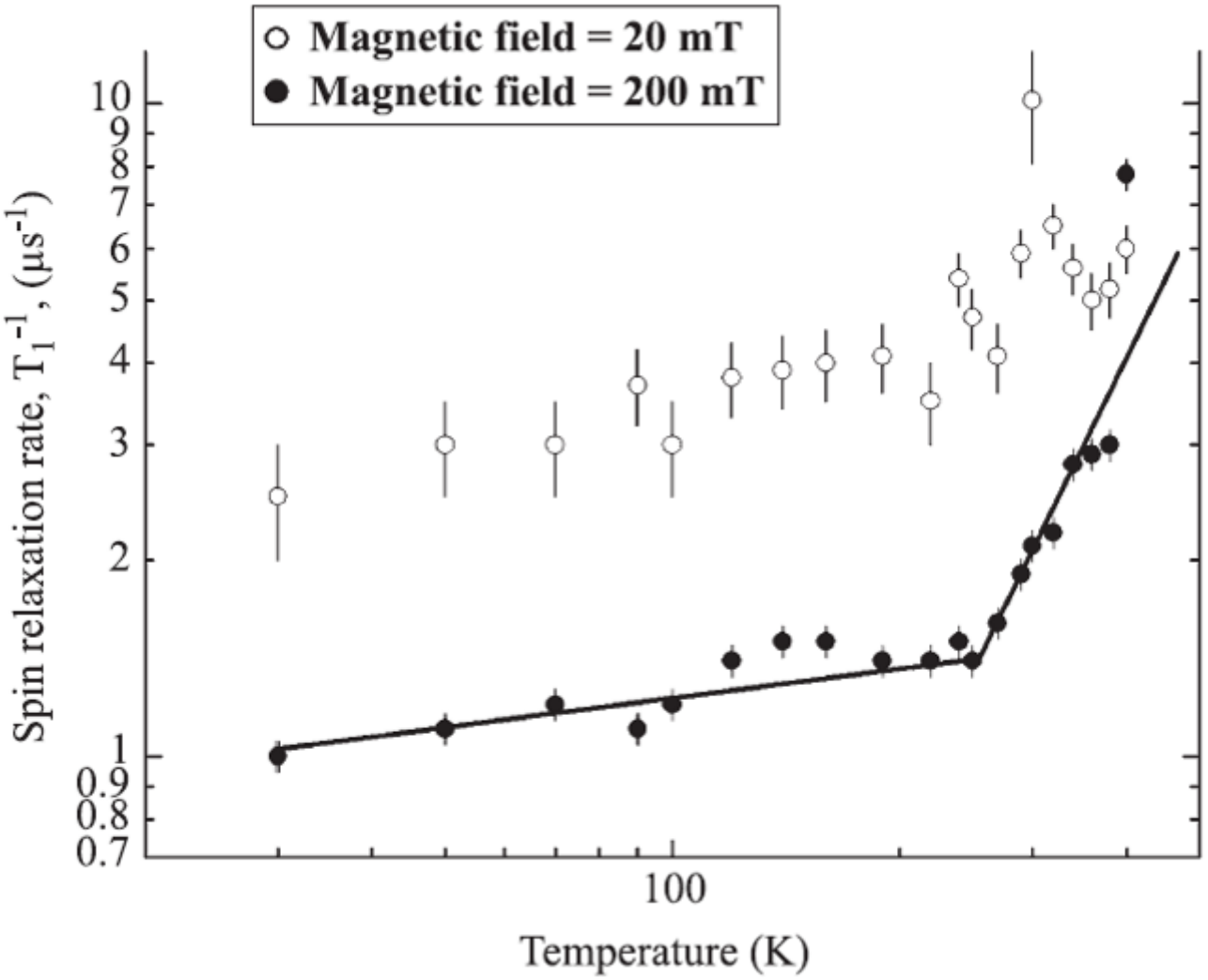

LF MSR in a ^{13}C diamond

Conclusions

1. The spin relaxation rate, T_1^{-1}, does have a power law behaviour, but this is due to a change in the nuclear hyperfine constant rather than the hop rate. As the temperature increases, the muonium localises. This could be the onset of the $Mu_T \rightarrow Mu_{BC}$ transition.
2. The hop rate is very high : $6 \times 10^{10} s^{-1}$. It is also almost constant in temperature over the range studied. This is consistent with previous conclusion of quantum diffusion.
3. Apart from this general agreement, the results of the LF measurements do not fully reconcile with the TF measurements.

Possible Mu_{BC} thermal ionisation

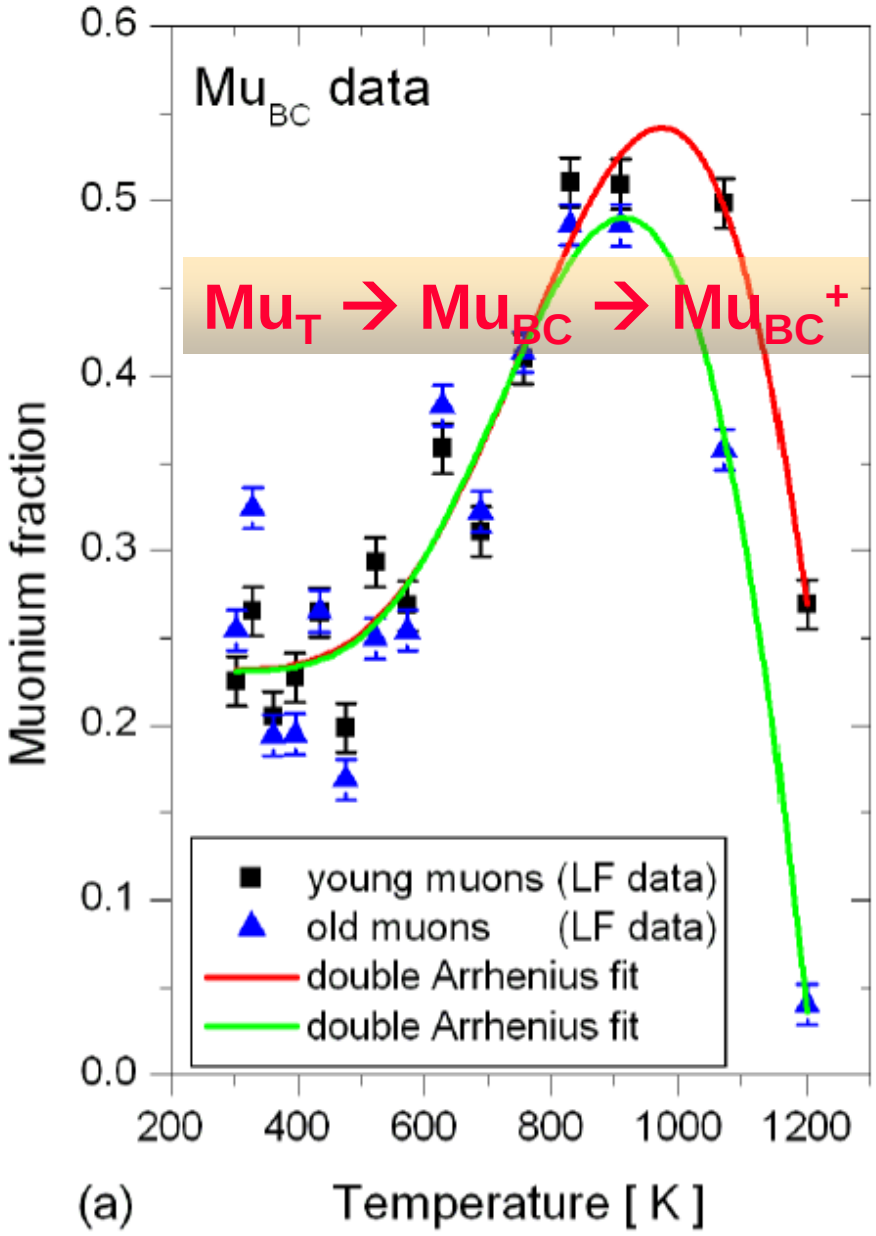

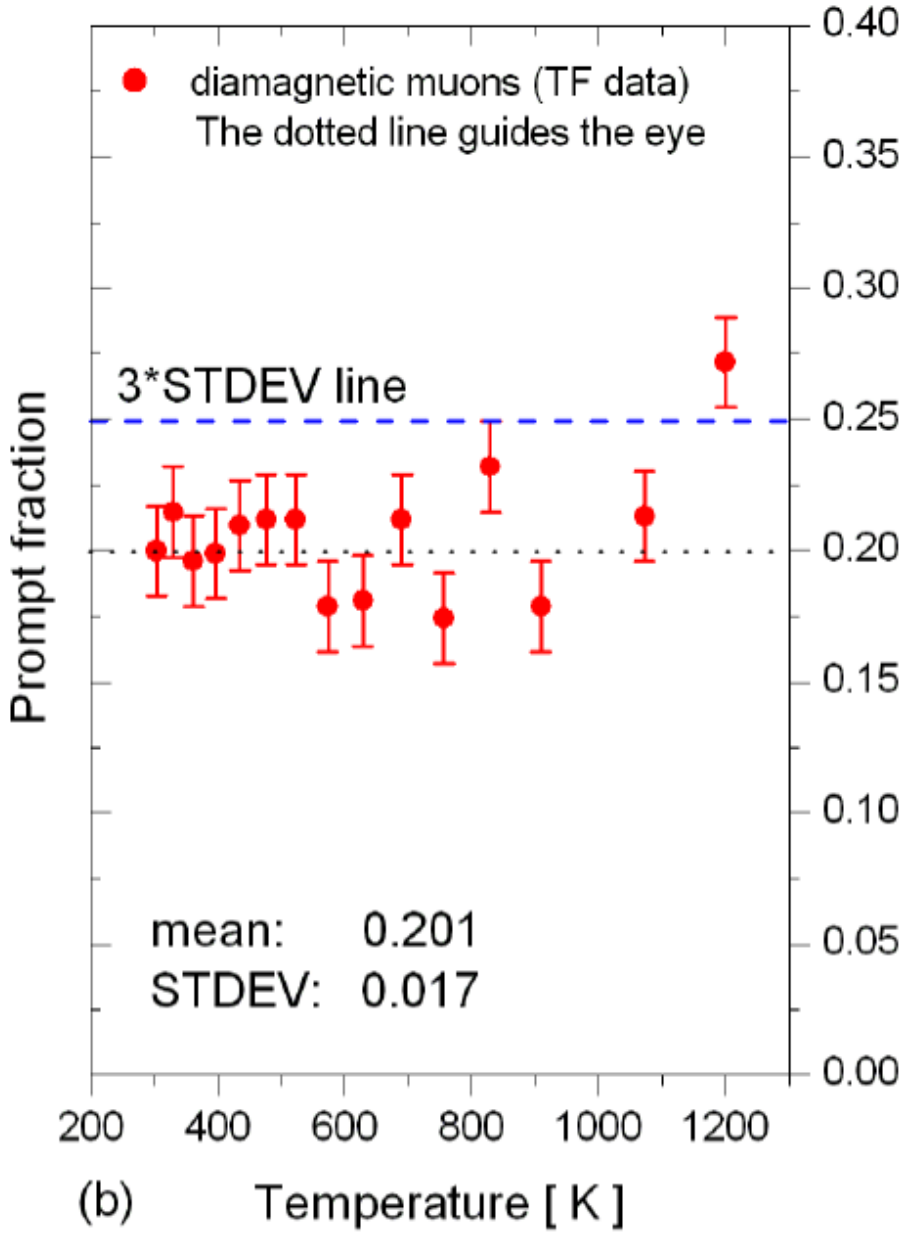

Possible Mu_{BC} thermal ionisation

Conclusions

1. $Mu_T \rightarrow Mu_{BC}$ transition observed in LF for the first time with the correct activation energy of 0.476eV.
2. The transition $Mu_T \rightarrow Mu_{BC}$ occurs faster than the trapping of Mu_T at nitrogen centres at high temperatures. This supports the idea that Mu_T must first localise before it can convert.
3. If Mu_{BC} is ionising, its rate is faster than $2 \times 10^8 s^{-1}$.
4. This would also imply the level of Mu_{BC} in the gap is 0.60 – 1.80 eV (dependant on data analysis model)
5. There is still the possibility (very small) that Mu_{BC} has become mobile, accounting for its depolarisation. (Recent measurement to higher T to check this).

MSR in Diamond

SH Connell, K Bharuth-Ram, S Cox

University of Johannesburg, Univ. of KwaZulu-Natal, Rutherford Appleton Lab

Electronic
Optical
Quantum